The Plant Cell, Vol. 22: 918–936, March 2010, www.plantcell.org

Endosome-Associated CRT1 Functions Early in *Resistance* Gene–Mediated Defense Signaling in *Arabidopsis* and Tobacco [W]

Hong-Gu Kang,[a] Chang-Sik Oh,[a] Masanao Sato,[b,1] Fumiaki Katagiri,[b] Jane Glazebrook,[b] Hideki Takahashi,[c] Pradeep Kachroo,[d] Gregory B. Martin,[a,e] and Daniel F. Klessig[a,2]

[a] Boyce Thompson Institute for Plant Research, Ithaca, New York 14853
[b] Department of Plant Biology, University of Minnesota, St. Paul, Minnesota 55108
[c] Department of Life Science, Tohoku University, Sendai 981-8555, Japan
[d] Department of Plant Pathology, University of Kentucky, Lexington, Kentucky 40546
[e] Department of Plant Pathology and Plant-Microbe Biology, Cornell University, Ithaca, New York 14853

Resistance **gene–mediated immunity confers protection against pathogen infection in a wide range of plants. A genetic screen for *Arabidopsis thaliana* mutants compromised for recognition of turnip crinkle virus previously identified CRT1, a member of the GHKL ATPase/kinase superfamily. Here, we demonstrate that CRT1 interacts with various resistance proteins from different structural classes, and this interaction is disrupted when these resistance proteins are activated. The *Arabidopsis* mutant *crt1-2 crh1-1*, which lacks CRT1 and its closest homolog, displayed compromised resistance to avirulent *Pseudomonas syringae* and *Hyaloperonospora arabidopsidis*. Additionally, resistance-associated hypersensitive cell death was suppressed in *Nicotiana benthamiana* silenced for expression of *CRT1* homolog(s). Thus, CRT1 appears to be a general factor for *resistance* gene–mediated immunity. Since elevation of cytosolic calcium triggered by avirulent *P. syringae* was compromised in *crt1-2 crh1-1* plants, but cell death triggered by Nt MEK2^{DD} was unaffected in *CRT1*-silenced *N. benthamiana*, CRT1 likely functions at an early step in this pathway. Genome-wide transcriptome analysis led to identification of *CRT1-Associated* genes, many of which are associated with transport processes, responses to (a)biotic stress, and the endomembrane system. Confocal microscopy and subcellular fractionation revealed that CRT1 localizes to endosome-like vesicles, suggesting a key process in resistance protein activation/signaling occurs in this subcellular compartment.**

INTRODUCTION

Plants are constantly challenged by a wide range of potential pathogens. However, successful pathogenesis leading to disease is the exception for these would-be pathogens, due to the multilayered nature of resistance in plants. In addition to preformed physical and chemical barriers, which serve as the first line of defense, plants recognize compounds containing molecular patterns common and unique to pathogens and other microbes (known as pathogen/microbe associated molecular patterns) and induce pathogen-associated molecular pattern-triggered immunity (PTI). Responses associated with PTI include increased cytosolic Ca^{2+} levels and activation of mitogen-activated protein (MAP) kinase cascades (reviewed in Schwessinger and Zipfel, 2008). Most highly adapted pathogens, however, have long overcome PTI by delivering effectors into host plants to suppress/target various plant defense components (reviewed in Birch et al., 2008; Block et al., 2008).

In turn, plants prevent infection by these pathogens by activating gene-for-gene resistance, also known as effector-triggered immunity (ETI). ETI was first described genetically as a highly specific resistance to a small number of pathogens; it involves a gene from the host plant and a cognate gene from the pathogen (Flor, 1971). The pathogen component involved in ETI was shown to be a pathogen-derived effector, previously termed avirulence factor, and the host counterpart was termed a Resistance (R) protein that presumably functions by recognizing the presence or activity of the pathogen effector(s) (Bent and Mackey, 2007). Contrary to early anticipation that R proteins would be receptors for pathogen effectors, very few R proteins, except for tomato (*Solanum lycopersicum*) Pto, *Arabidopsis thaliana* RRS1, rice (*Oryza sativa*) Pi-ta, and flax (*Linum usitatissimum*) L, have been shown to directly recognize their corresponding effector (Scofield et al., 1996; Tang et al., 1996; Jia et al., 2000; Deslandes et al., 2003; Dodds et al., 2006). Instead, a large number of R proteins appear to detect pathogen effectors indirectly, by sensing perturbations in other host proteins that are targeted by pathogen-derived effectors; this is known as the guard hypothesis (Dangl and Jones, 2001). For instance, the *Arabidopsis* R proteins RPM1 and RPS2 guard host

[1] Current address: Okazaki Institute for Integrative Bioscience, National Institutes of Natural Sciences, Myodaiji, Okazaki 444-8787, Japan.
[2] Address correspondence to dfk8@cornell.edu.
The author responsible for distribution of materials integral to the findings presented in this article in accordance with the policy described in the Instructions for Authors (www.plantcell.org) is: Daniel F. Klessig (dfk8@cornell.edu).
[W] Online version contains Web-only data.
www.plantcell.org/cgi/doi/10.1105/tpc.109.071662

protein RIN4, which is targeted by *Pseudomonas syringae* effector proteins AvrRPM1/AvrB and AvrRPT2, respectively, while RPS5 monitors PBS1 (Mackey et al., 2002, 2003; Axtell and Staskawicz, 2003; Shao et al., 2003). Alterations, including phosphorylation and degradation, of these guarded host proteins lead to constitutive defense responses, including the hypersensitive response (HR), a form of programmed cell death that helps restrict the pathogen's proliferation in host plants. Interestingly, the molecular changes underlying these ETI-associated responses are generally similar to those triggered by PTI but are more robust and rapid (Tao et al., 2003).

A large number of *R* genes have been identified, and most encode proteins containing nucleotide binding (NB) and leucine-rich repeat (LRR) domains (reviewed in Martin et al., 2003). The NB-LRR group is further divided into two subgroups that contain either a coiled-coil domain (CC-NB-LRR) or a motif resembling the *Drosophila melanogaster* Toll and human interleukin 1 receptor (TIR-NB-LRR) at their N terminus. Several components that are required for fully functional R protein–mediated resistance also have been identified, including EDS1 (for enhanced disease susceptibility 1), NDR1 (for non-race-specific disease resistance 1), RAR1 (for required for Mla12 resistance 1), SGT1 (for suppressor of the G_2 allele of *skp1*), and HSP90 (for heat shock protein 90). Each of these proteins influences the activity of a different spectrum of R proteins (reviewed in Bent and Mackey, 2007). For example, EDS1 and NDR1 are mostly required for resistance mediated by TIR-NB-LRR and CC-NB-LRR, respectively (Aarts et al., 1998). By contrast, RAR1, SGT1, and HSP90 mediate resistance triggered by R proteins belonging to both the TIR-NBS-LRR and CC-NBS-LRR groups (reviewed in Shirasu and Schulze-Lefert, 2003; Belkhadir et al., 2004). RAR1, SGT1, and HSP90 have been shown to physically interact with a wide range of R proteins, raising the possibility of their involvement in an R protein complex. Since RAR1 and HSP90 are crucial for the stability of some R proteins, they are proposed to function as (co) chaperones (Hubert et al., 2003, 2009; Lu et al., 2003), while SGT1 may be involved in ubiquitin-mediated proteolysis (Azevedo et al., 2002, 2006). However, despite the growing number of R protein–associated components, the activation mechanism of R proteins upon pathogen recognition is still unclear.

The *Arabidopsis* R protein HRT of the Di-17 ecotype indirectly recognizes the coat protein (CP) of turnip crinkle virus (TCV; Cooley et al., 2000; Zhao et al., 2000). The identity of the host protein(s) targeted by CP was initially proposed to be TCV-interacting protein (TIP), which is a NAC transcription factor (Ren et al., 2000, 2005). However, the recent demonstration that TCV resistance is unaltered in TIP-deficient *Arabidopsis* suggests that TIP is not the guardee protein (Jeong et al., 2008). Through a genetic screen for mutants with compromised HRT-mediated resistance, we previously identified *crt1* (for compromised recognition of TCV-CP 1; Kang et al., 2008). CRT1 is an ATPase carrying a GHKL ATPase motif (Dutta and Inouye, 2000). Interestingly, CRT1 physically interacts with several R proteins besides HRT, raising the possibility that CRT1 is a general factor in *R* gene–mediated resistance. Consistent with this possibility, cell death triggered by other R proteins, including ssi4 (Shirano et al., 2002) and RPS2 (Mindrinos et al., 1994), is compromised by the *crt1* mutation or silencing of the *CRT1* family members (Kang et al., 2008).

In this study, we used T-DNA insertion mutants of *CRT1* and/or its homolog *CRH1* in *Arabidopsis* and virus-induced gene silencing (VIGS) of the *CRT1* homolog(s) in *Nicotiana benthamiana* to demonstrate that the CRT1 family functions in resistance mediated by a wide range of R proteins. Note that *Arabidopsis* CRT1 homologs have been renamed CRH1-6 instead of CRT1-H1-6, the nomenclature that was previously used (Kang et al., 2008). Interestingly, the interaction between CRT1 and various R proteins appears to be disrupted when the R proteins are in an active state, caused either by recognition of their corresponding pathogen effector or by *R* gene overexpression, which can lead to autonomous activation. These results suggest that the CRT1–R protein interaction is dynamic and may be associated with R protein activation. Characterization of the *CRT1*-associated transcriptome also is presented, and placement of CRT1 in the *R* gene–mediated signal transduction pathway is discussed.

RESULTS

CRT1 Physically Associates with a Wide Range of R Proteins and HSP90

CRT1 was previously shown to be required for HRT-mediated resistance to TCV in *Arabidopsis* and, based on coimmunoprecipitation (co-IP) analysis, to physically associate with HRT and the R proteins RPS2, Rx, and SSI4 (Kang et al., 2008). Since the latter result suggested that CRT1 is a general R protein–interacting protein, we tested its ability to interact with six additional R proteins, RCY1, RPP8, RPP8c, RPM1, and SNC1 from *Arabidopsis* and Pto from tomato (Figure 1A). As a first step, these HA-tagged R proteins were transiently coexpressed with Myc-tagged CRT1 in *N. benthamiana*. Overexpression of RCY1 (Figure 2A) and RPM1 induced spontaneous cell death in *N. benthamiana*, thereby potentially reducing their expression levels; this phenomenon was previously observed with RPS2 (Kang et al., 2008). To circumvent this problem, the mutant genes *rcy1-3* (Sekine et al., 2006), *RPM1ΔC*, and, as a positive control, *RPS2m* (R2M4; K188L; Tao et al., 2000) were expressed instead of their wild-type counterparts. Note that RPS2m and RPM1ΔC only accumulated to very low levels (Figure 1A, panel iii, lanes 3 and 7); however, their expression was confirmed when triple the amount of the same protein extracts used in Figure 1A was used for immunoblot (IB) analysis with αHA (see Supplemental Figure 1A online). As previously reported, IB analysis with αMyc revealed a doublet of CRT1, suggesting that this protein is posttranslationally modified (Figure 1A, panel ii). Co-IP analysis indicated that all six R proteins, as well as the positive controls HRT and RPS2m, interact with CRT1 (Figure 1A, panel i). By contrast, the negative control green fluorescent protein (GFP) did not exhibit any interaction. While most of the R proteins tested belong to the CC-NB-LRR class, SNC1 and Pto belong to the TIR-NB-LRR and cytosolic kinase classes, respectively. Thus, these results indicate that CRT1 interacts directly or indirectly with R proteins from at least three different classes.

Since RAR1, SGT1, and HSP90 physically interact with a wide range of R proteins, we tested whether CRT1 also interacts with

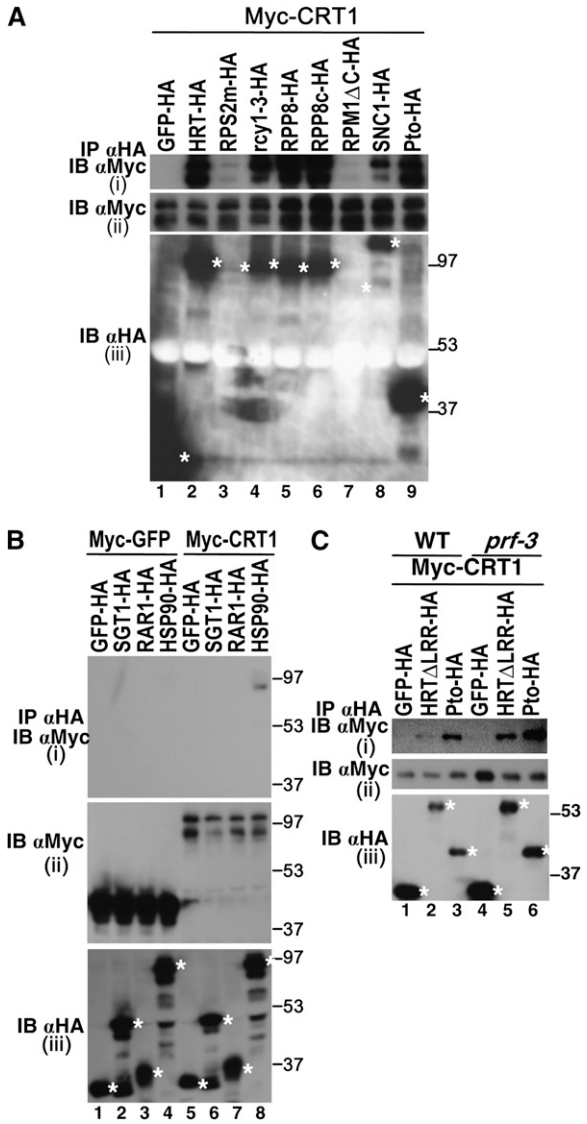

Figure 1. CRT1 Interacts with a Wide Range of R Proteins and HSP90.

Soluble extracts were subjected to 12% SDS-PAGE followed by IB analysis with the indicated antibodies or co-IP with αHA-agarose beads, followed by IB. Size markers are shown on the right of the panels in kilodaltons. For each, at least three independent experiments were performed with similar results. Input (ii and iii) and IP (i) proteins were analyzed using IB with αHA (iii) and αMyc (i and ii). Asterisks indicate the expected sizes of HA-tagged proteins.
(A) *Myc-CRT1*, *HA-tagged R*, or *HA-tagged GFP* genes were transiently overexpressed in *N. benthamiana*.
(B) *Myc-CRT1*, *Myc-GFP*, *GFP-HA*, *SGT1-HA*, *RAR1-HA*, and *HSP90-HA* genes were transiently overexpressed in *N. benthamiana*.
(C) IB and co-IP analyses were performed using wild-type or *prf-3* tomato protoplasts transfected with the indicated genes.

them. Co-IP analysis revealed modest interaction between CRT1 and HSP90 and little or no interaction with either SGT1 or RAR1 (Figure 1B). Interestingly, the lower band of the CRT1 doublet exhibited better interaction with HSP90 than the higher, although the significance of this observation is unknown.

Activated R Proteins Show Little Physical Association with CRT1

To assess whether an R protein's activation status affects its ability to interact with CRT1, we monitored the interaction between CRT1 and either *RCY1*, whose overexpression triggered autonomous cell death in *N. benthamiana*, or *rcy1-3* or *rcy1-6*, mutated versions of this gene whose overexpression does not trigger cell death (Figure 2A; Sekine et al., 2006). Co-IP analysis revealed that CRT1 interacted with rcy1-3 and rcy1-6, but not with RCY1 (Figure 2B). Combined with our previous demonstration that CRT1 fails to interact with RPS2, RPM1, or ssi4, which all trigger autonomous cell death (Kang et al., 2008; data not shown), this result raised the possibility that CRT1 only interacts with R proteins in their inactive state. To further assess this possibility, we monitored CRT1's ability to interact with HRT in the presence or absence of HRT's corresponding effector, TCV CP (generated by agroinfiltrating the TCV genome under the cauliflower mosaic virus 35S promoter). As expected, coexpression of *HRT* and *CP* triggered a visible HR at 3 d after infection (DAI), whereas coexpression with a mutant TCV (*mTCV*), which precludes HRT recognition (D4N in CP; Zhao et al., 2000), did not (Figure 2C). Co-IP analysis revealed that at all time points examined, including those prior to the appearance of a visible HR, the HRT–CRT1 interaction was considerably reduced by the presence of wild-type CP compared with mutant CP (mTCV) or GFP (Figure 2D, panel i). Some reduction in the HRT–CRT1 interaction can be attributed to decreased levels of HRT in plants expressing the wild-type CP (Figure 2D, panel iii). However, comparison of samples taken at 2 DAI, when HRT expression was comparable in plants expressing GFP, TCV, or mTCV suggests that co-IP of the lower band of CRT1 was preferentially reduced (cf. lanes 1, 4, and 7 in panel iii, Figure 2D). This result suggests that the decline in HRT–CRT1 interaction, particularly for the lower band of the CRT1 doublet, correlates with activation of HRT via its corresponding effector, TCV CP.

Interaction of CRT1 with Pto Is Independent of Prf

In tomato, Pto works in conjunction with the CC-NB-LRR R protein Prf to confer resistance to *P. syringae* pv *tomato* (*Pst*) carrying *AvrPto* or *AvrPtoB* (Martin et al., 1993; Salmeron et al., 1996; Kim et al., 2002). Interestingly, Pto was recently shown to physically associate with Prf (Mucyn et al., 2006), raising the possibility that the Pto–CRT1 interaction occurs indirectly through the *N. benthamiana* Prf homolog. To test this possibility, CRT1 and Pto were transiently expressed in tomato protoplasts generated from either the mutant RG-*prf3*, which expresses no detectable Prf protein (Mucyn et al., 2006) or wild-type plants. The HRT variant (HRTΔLRR), which is devoid of the LRR domain and was previously shown to interact with CRT1 (Kang et al., 2008), was used as a positive control. Co-IP analysis indicated that CRT1 associated with Pto or HRTΔLRR in RG-*prf-3* as well as in wild-type protoplasts (Figure 1C), suggesting that the Pto–CRT1 interaction does not require Prf. CRT1 expressed in tomato protoplasts migrated as a single band that corresponds to the lower band of the CRT1 doublet in *N. benthamiana* (see Supplemental Figure 1B online); this result suggests that tomato

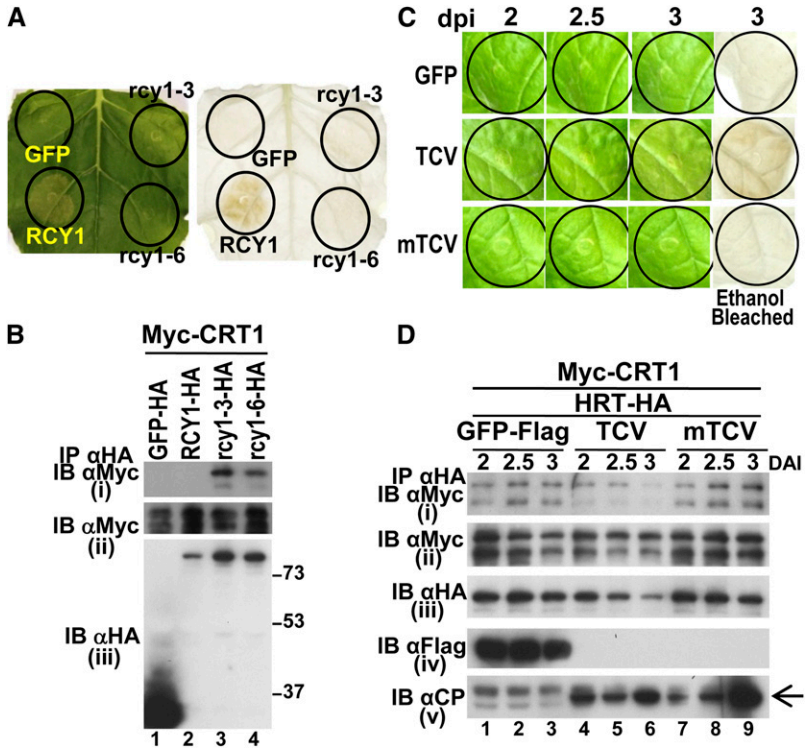

Figure 2. CRT1 Displays Little Interaction with Activated R Proteins.

(A) *RCY1*, *rcy1-3*, *rcy1-6*, and *GFP* were transiently overexpressed for 3 d in *N. benthamiana.* Infiltrated areas were circled. To better visualize cell death, the leaf was bleached in ethanol (right panel).
(B) Co-IP was performed on extracts from *N. benthamiana* leaves in which all the genes in **(A)** were coexpressed with *Myc-CRT1*.
(C) *HA-HRT* and *Myc-CRT1* were coexpressed in *N. benthamiana* together with wild-type *TCV*, its mutant (*mTCV*), or *GFP-Flag*. Photographs were taken at the indicated days after infiltration (dpi). The right column shows leaves 3 d after infiltration after bleaching with ethanol.
(D) Co-IP was performed with all of the samples shown in **(C)**. Input (ii to v) and IP (i) proteins were analyzed using IB with αHA (iii), αMyc (i and ii), αFlag (iv), or αCP (v). The arrow indicates the expected size of TCV CP.
In **(A)** to **(D)**, three independent experiments were performed with similar results.

protoplasts and *N. benthamiana* plants posttranslationally modify CRT1 differently.

R Gene–Mediated Resistance to *P. syringae* and *Hyaloperonospora arabidopsidis* Is Compromised in *crt1-2 crh1-1*

To further characterize the *CRT1* family, *Arabidopsis* T-DNA insertion mutants for *CRT1* (*crt1-2*; SAIL_893_B06) or its closest homologs, *CRH1* (*crh1-1*; SALK_072774) and *CRH2* (*crh2-1*; SALK_000009), were obtained from the ABRC. The *crt1-2* and *crh1-1* mutants largely displayed wild-type morphology (see Supplemental Figure 2A online). By contrast, the *crh2-1* mutation appears to be lethal since about one-quarter of the seeds from self-pollinated plants heterozygous for this mutation were aborted (see Supplemental Figure 2B online) and no homozygous *crh2-1* lines were recovered in the following generation. Thus, only *crt1-2* and *crh1-1* were studied further.

CRT1 family members were previously shown to be functionally redundant (Kang et al., 2008); thus, a *crt1-2/crh1-1* double mutant was generated (*crt1-2 crh1-1*). Since *CRT1* and *CRH1* are tightly linked (T-DNA insertion sites in *crt1-2* and *crh1-1* are ~4 kb apart), we used a previously described approach to select for meiotic recombinants between T-DNA insertions in the *crt1-2* and *crh1-1* mutants that contained selectable markers conferring resistance to basta or kanamycin, respectively (Barth and Jander, 2006). Following identification of meiotic recombinants carrying both resistance markers, RT-PCR confirmed that the *crt1-2 crh1-1* double knockout (KO) lacked expression of both genes, while the *crt1-2* and *crh1-1* single KO mutants displayed little, if any, expression of *CRT1* or *CRT1-h1*, respectively (see Supplemental Figure 2C online). Note that *crt1-2* and *crh1-1* are likely single insertion mutants as their heterozygous progeny displayed single gene segregation in the following generation ($\chi^2 < 0.05$). In addition, the extremely low frequency of meiotic recombinants between the T-DNA insertion sites in *crt1-2* and *crh1-1* (1 out of >25,000) suggests that insertion of T-DNA in additional gene(s) is unlikely.

We previously reported that RPS2-mediated HR development was delayed by partial silencing of *CRT1*, *CRH1*, and *CRH2*, whereas RPS2-mediated resistance was unaffected (Kang et al., 2008). Since the unaltered resistance in these plants could have

been due to inefficient gene silencing, the double and single KO mutants were monitored for resistance to *Pst* carrying *AvrRpt2* (*Pst AvrRpt2*). Higher levels of bacterial growth were detected in the single and double KO mutants compared with wild-type plants at 2 DAI (Figure 3A); this result suggests that *RPS2*-mediated resistance was compromised by the loss of *CRT1* and/or *CRH1*. Consistent with this finding, wild-type plants displayed little to no disease symptoms at 5 DAI, whereas the three KO mutants developed patchy chlorosis (Figure 3A, bottom panel). These symptoms, however, were not as severe as those on *rps2*, in which the cognate *R* gene is nonfunctional.

RPM1-mediated resistance against *Pst* carrying *AvrRpm1* (*Pst AvrRpm1*) also was assessed, since RPM1 physically associates with CRT1 (Figure 1A). Compared with the wild type, *crt1-2 crh1-1* plants supported much more growth of *Pst AvrRpm1*, and they exhibited extensive disease symptoms (Figure 3B). These results argue that *RPM1*-mediated resistance also is compromised in the double KO mutant, although it is not fully suppressed since even greater levels of bacterial growth and disease symptoms were observed in susceptible *rpm1* plants. Resistance in *crt1-2*, as indicated by pathogen growth, was only marginally compromised. To assess whether compromised RPM1-mediated resistance in the *crt1-2 crh1-1* background was due to RPM1 instability, a transgenic RPM1-Myc–tagged line was generated in the double KO background. IB analysis with α-Myc showed that RPM1-Myc accumulation was comparable in *crt1-2 crh1-1* and wild-type plants (see Supplemental Figure 3 online).

The interaction between CRT1 and RPP8, an R protein identified in the *Arabidopsis* ecotype Landsberg *erecta* that confers resistance to *H. arabidopsidis* isolate Emco5 (McDowell et al., 1998), prompted us to test whether resistance to this oomycete pathogen also was altered in the double and single KO plants. It should be noted that in the Columbia-0 (Col-0) ecotype, resistance to Emco5 is mediated not by the RPP8 homolog, RPP8c, but rather by the RPP31 locus (McDowell et al., 2005), whose identity is currently under investigation (J.M. McDowell, personal communication). As previously reported, plants from the wild-type Landsberg *erecta* and Col-0 ecotypes were resistant to *H. arabidopsidis* Emco5 and developed few sporangiophores (Figure 3C). By contrast, plants from the wild-type Wassilewskija ecotype were very susceptible, with the majority supporting 21 or more sporangiophores per leaf pair. In comparison to wild-type Col-0, *crt1-2 crh1-1* supported considerably more growth of *H. arabidopsidis* Emco5, and the single KO mutants showed an intermediate resistance between wild-type Col-0 and the double KO mutant (Figure 3C; see Supplemental Figure 4 online). Together, these results suggest that the CRT1 family is necessary for full *R* gene–mediated resistance to an oomycete as well as a bacterial pathogen.

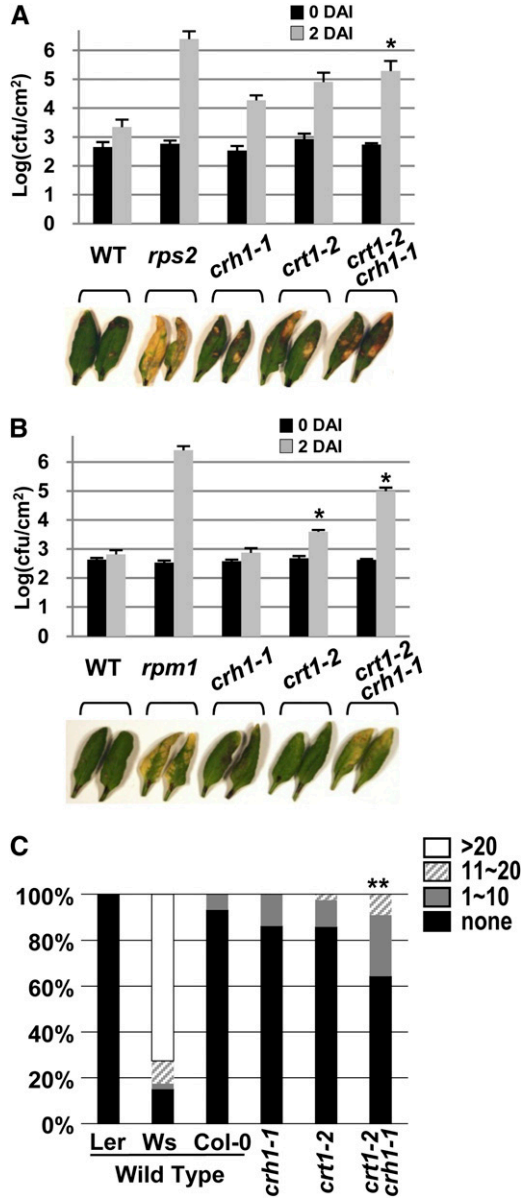

Figure 3. The *crt1-2 crh1-1* Mutant Shows Compromised *R* Gene–Mediated Resistance to Bacterial and Oomycete Pathogens.

(A) and **(B)** Following infection with 10^5 colony-forming units (cfu)/mL *Pst* carrying *AvrRpt2* **(A)** or *AvrRpm1* **(B)**, bacterial growth in 4-week-old wild type, *rps2*, *rpm1*, and the single and double *crt1-2 crh1-1* T-DNA mutants was measured at 0 and 2 DAI; the mean ± SE (n = 4) is presented. Three independent experiments were performed with similar results. Statistical difference from the wild type is indicated;*P < 0.05 (*t* test).

(C) Eight days after infection with *H. arabidopsidis* Emco5, disease levels were scored in 3-week-old plants from the three wild-type ecotypes and the mutants by counting the number of sporangiophores on the third pair of leaves. The percentage in each category was calculated from analysis of three independent experiments with 42 plants or more for each genotype. Statistical difference from the wild type (Col-0) in plants with any sporangiophore(s) is indicated; **P < 0.01 (Fisher's exact test).

Silencing of a *CRT1* Homolog(s) in *N. benthamiana* Compromised Development of Cell Death Triggered by Pto or RPM1, but Not by a Constitutively Activated MAP Kinase Kinase

N. benthamiana plants are highly amenable to loss-of-function studies due to a well-characterized VIGS system (Goodin et al., 2008). To use VIGS in *N. benthamiana*, a search for CRT1 homologs was undertaken using the GenBank database and the

Solanaceae genomics network. The database search, under a very stringent E value of e^{-100} or less, revealed that *Arabidopsis CRT1* (At *CRT1*) has homologs in several plant species, ranging from tomato, grape (*Vitis vinifera*), rice, and maize (*Zea mays*) to moss (Figure 4A). Using sequence information from tomato (Sl CRT1; annotated as *Arabidopsis* At4g36290 homolog; At4g36290 is the locus name for At CRT1), *CRT1*'s homolog was amplified from *N. benthamiana* cDNA; it has 70.2% amino acid identity to At CRT1 and was designated Nb CRT1. A tobacco rattle virus (TRV)-based vector (Liu et al., 2002a) carrying Nb *CRT1* (TRV-Nb-*CRT1*) or, for the negative control, the TRV vector lacking any target sequence (TRV-*EV*) was then used to inoculate *N. benthamiana.* RT-PCR analysis revealed that *CRT1* expression in the TRV-Nb-*CRT1*–inoculated plants was highly reduced compared with that in the TRV-*EV*–inoculated plants (see Supplemental Figure 5 online).

To examine if CRT1 is involved in Pto-mediated resistance responses, *Pto* was expressed together with its corresponding effector, *AvrPto* or *AvrPtoB*$_{1\text{-}387}$, in either TRV-*EV*– or TRV-Nb-*CRT1*–inoculated plants to trigger an HR. Note that the truncated mutant AvrPtoB$_{1\text{-}387}$ was used because wild-type AvrPtoB suppresses cell death in *N. benthamiana* (Abramovitch et al., 2003). Pto-mediated HR triggered by AvrPto or AvrPtoB$_{1\text{-}387}$ was compromised in TRV-Nb-*CRT1*–inoculated plants compared with the TRV-*EV* control plants (Figures 4B and 4C), suggesting that CRT1 is required for full Pto-mediated HR.

Since RPM1-mediated resistance was compromised in *Arabidopsis crt1-2 crh1-1*, we examined whether cell death triggered by AvrB, another effector protein for RPM1, was affected in Nb *CRT1*–silenced *N. benthamiana.* Expression of *AvrB* in *N. benthamiana* triggers cell death, presumably via an RPM1 homolog (Schechter et al., 2004). This AvrB-triggered cell death in *N. benthamiana* expressing TRV-Nb-*CRT1* was partially suppressed in comparison to that exhibited by TRV-*EV* control plants (Figures 4B and 4C), arguing that resistance responses mediated by an RPM1 homolog in *N. benthamiana* are also influenced by CRT1.

Whether CRT1 is required for cell death triggered by a signaling component downstream of an *R* gene was then tested. Nt MEK2 is the second component of a three-step MAP kinase cascade, and it is one of the downstream components in Pto-mediated resistance in *N. benthamiana* (del Pozo et al., 2004). The constitutively active mutant of Nt MEK2, Nt MEK2^{DD}, triggers spontaneous HR-like cell death (Yang et al., 2001). Interestingly, comparable levels of cell death triggered by Nt MEK2^{DD} were observed in TRV-Nb-*CRT1*– and TRV-*EV*–inoculated plants (Figures 4B and 4C). This result suggests that CRT1 functions upstream of Nt MEK2 in the cell death signaling pathway triggered by Nt MEK2^{DD}.

Cytosolic Ca^{2+} Influx in Response to Avirulent *P. syringae* Was Compromised in *crt1-2 crh1-1*

Calcium (Ca^{2+}) is a second messenger whose sustained elevation following pathogen or elicitor treatment has been associated with the induction of plant defense responses, including activation of MAP kinases (Grant et al., 2000; Lecourieux et al., 2002). To assess whether CRT1 family members are required for

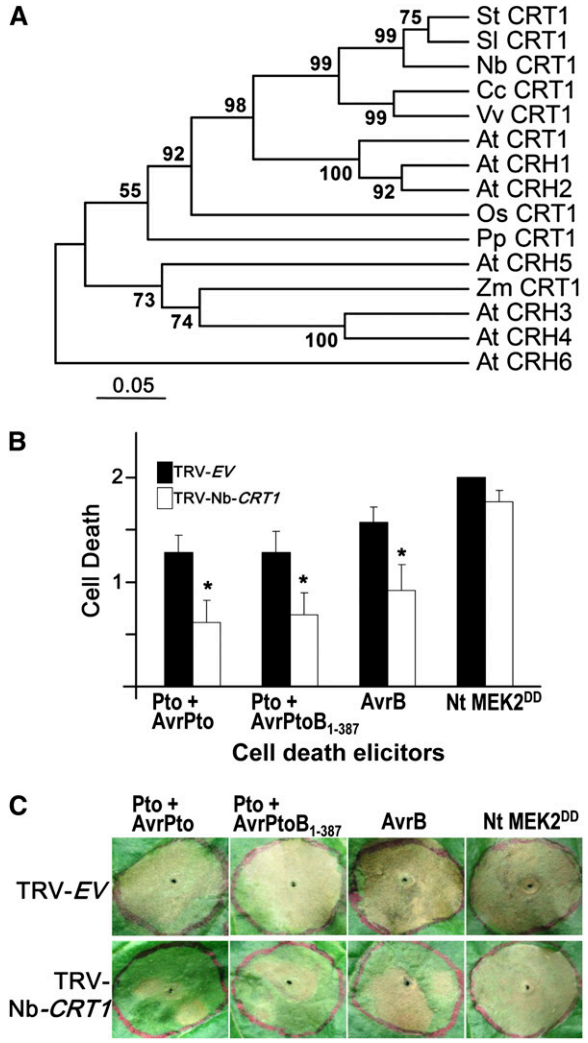

Figure 4. Silencing the *CRT1* Gene in *N. benthamiana* Compromised Cell Death Mediated by Pto or RPM1.

(A) Phylogenetic comparison of non-*Arabidopsis* CRT1 homologs with E values of e^{-100} or less and all the *Arabidopsis* CRT1 family members (At CRT1 and At CRH1-6). Phylogenetic analysis was conducted using MEGA 4.1. Accession numbers for non-*Arabidopsis* CRT1 homologs are as follows: Sl CRT1 (tomato; SGN-U349134), St CRT1 (potato; SGN-U273098), Nb CRT1 (GQ855284), Cc CRT1 (coffee; SGN-U357963), Vv CRT1 (grape; CAO48278), Os CRT1 (rice; AAK70637), Pp CRT1 (moss; XP_001762322), and Zm CRT1 (maize; ACG47873).

(B) The *CRT1* gene was silenced by TRV-based VIGS in *N. benthamiana*; the TRV-empty vector (TRV-*EV*) was used as a negative control. Five weeks after infection with TRV-Nb-*CRT1* or TRN-*EV*, cell death elicitors were transiently overexpressed. Cell death (CD) was scored at 3 DAI after expression of AvrB or Nt MEK2^{DD} or 4 DAI with Pto and either AvrPto or AvrPtoB$_{1\text{-}387}$ using the following scoring system: 2 for full CD, 1 for partial CD, and 0 for no CD. In each experiment, two to three leaves were infiltrated on each of three to four independent silenced plants. The results shown are representative of three independent experiments; the mean ± SE (n = 13) is presented. Statistical difference between TRV-*EV* and TRV- Nb-*CRT1* is indicated; *P < 0.05 (t test).

(C) Representative photos for each CD elicitor in TRV-*EV* or TRV- Nb-*CRT1* plants were taken at 3 DAI (4 DAI for Pto).

resistance-associated increases in cytosolic Ca^{2+} levels, *crt1-2 crh1-1* and wild-type plants were transformed with the *Aequorin* gene, which encodes a bioluminescent protein sensitive to Ca^{2+} (Knight and Knight, 1995). As was previously reported (Grant et al., 2000), wild-type plants expressing Aequorin exhibited a sustained elevation of cytosolic Ca^{2+} that peaked ~2.5 h after infection with *Pst AvrRpm1* (Figure 5A). By contrast, the increase in cytosolic Ca^{2+} in *Aequorin*-expressing *crt1-2 crh1-1* plants inoculated with *Pst AvrRpm1* was less vigorous and peaked at ~2 h after infection (Figure 5A). No sustained elevation of Ca^{2+} levels was detected in *Aequorin*-expressing wild-type or *crt1-2 crh1-1* plants that received a mock inoculation or were infected with virulent *Pst*; indeed, their Ca^{2+} signatures were comparable. The fold of Ca^{2+} induction following each treatment was averaged from the second sustained peak and the preceding trough (Figure 5B). *crt1-2 crh1-1* consistently exhibited suppressed induction of Ca^{2+} elevation by *Pst AvrRpm1* compared with that in the wild type in four independent experiments (Figure 5B). The fold of induction for mock was not included as it had no obvious trough corresponding to those from pathogen treatments. These data suggest that the CRT1 family functions upstream of Ca^{2+} accumulation in RPM1-mediated signal transduction.

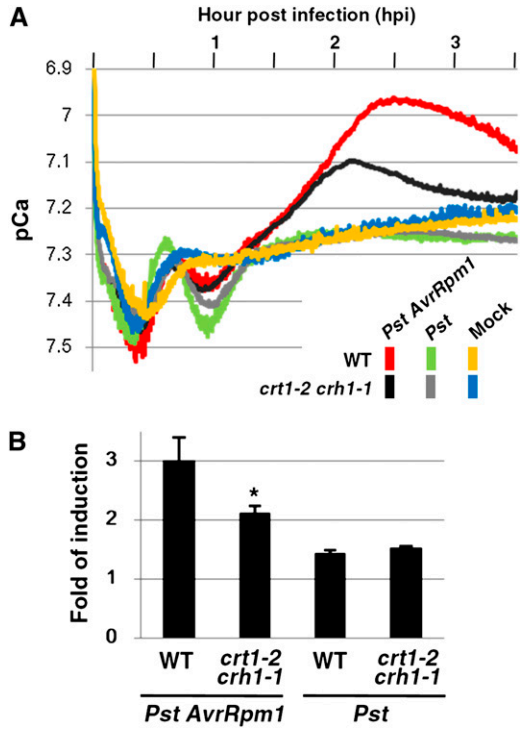

Figure 5. RPM1-Dependent Elevation of Cytosolic Calcium Was Compromised in *crt1-2 crh1-1*.

(A) Luminescence was measured in 3-week-old wild type and *crt1-2 crh1-1* expressing the *Aequorin* transgene following treatment with *Pst*, *Pst AvrRpm1*, or buffer only (mock). For infection 10^8 cfu/mL of *Pst* or *Pst AvrRpm1* was used. Measurements were integrated every 10 s for 210 min.

(B) Average fold of induction (±SE) was calculated from at least four independent experiments. *$P < 0.05$ (*t* test).

CRT1 Is Localized in Endosomes Displaying Rapid Cytosolic Streaming

To gain insights into CRT1 function, its subcellular location was investigated using transient expression of a *GFP-CRT1* fusion gene in *N. benthamiana*. Confocal microscopy revealed that GFP-CRT1 primarily resides within endocytotic vesicle-like structures of heterogeneous size, also known as endosomes (Figure 6). The location of GFP-CRT1 was further investigated by comparing it with red fluorescent protein (Shaner et al., 2004) tagged markers (Nelson et al., 2007) for mitochondria (yeast cytochrome oxidase subunit IV), Golgi complexes (soybean [*Glycine max*] α-1,2-mannosidase I), or peroxisomes (peroxisome targeting sequence 1). GFP-CRT1 generally showed little overlap with the Golgi and mitochondria markers, although occasional overlap was observed (Figures 6A and 6B, indicated by arrows). Interestingly, a modest number of CRT1-containing vesicles, particularly larger ones, overlap with the peroxisomal marker, suggesting that a subset of CRT1 localizes to peroxisomes (Figures 6C and 6D; panels in [D] are a higher magnification from an independent experiment). Moreover, GFP-CRT1–containing endosomes and peroxisomes displayed rapid cytoplasmic streaming (see Supplemental Movie 1 online). Note that peroxisomes showed significantly weaker fluorescence when they overlapped with GFP-CRT1 (Figures 5C and 5D, indicated by arrows). This may be due to interference between the two proteins localized in the same vesicle.

To complement these microscopy studies, the location of CRT1 was assessed in plasma membrane (PM) and endomembrane fractions separated via an aqueous two-phase purification strategy (Larsson et al., 1987). To this end, *crt1-2 crh1-1* plants containing a *Myc-CRT1* transgene were generated; overexpression of *Myc-CRT1* restored resistance against *Pst AvrRpm1* (see Supplemental Figure 6 online), suggesting that Myc-CRT1 is functional. Following aqueous two-phase separation of membranes from these plants, IB was performed using αMyc as well as antibodies for V-ATPase (a marker for the vacuole) and H^+ATPase (a marker for the PM) to monitor purity of the fractions (Reuveni et al., 2001; Page et al., 2009). Myc-CRT1 was predominantly detected in the endomembrane fractions of mock- and *Pst*-inoculated *crt1-2 crh1-1 Myc-CRT1* plants (Figure 7A). Similar analyses using either wild-type or *crt1-2 crh1-1* plants containing an *RPM1-Myc* transgene revealed that RPM1-Myc also was predominantly located in the endomembranes, regardless of mock or *Pst* inoculation (Figure 7B).

Two-step differential centrifugation at 13,000 and 100,000*g* was then performed to fractionate organelles/vesicles based on size and density (Nagahashi and Hiraike, 1982). Consistent with the heterogeneous size of vesicles carrying CRT1, Myc-CRT1 was enriched in both the 13,000*g* (p13) and the 100,000*g* (p100) pellet fractions (Figure 7C). The vacuolar marker V-ATPase also was detected in both of these fractions, whereas the PM marker H^+ATPase was primarily detected in the p100 fraction. Interestingly, RPM1-Myc displayed a similar distribution as Myc-CRT1 and V-ATPase, corroborating the possibility that CRT1 and RPM1 reside in endomembranes. In comparison to our results, Boyes et al. (1998) previously classified RPM1 as a PM protein. They did note the presence of RPM1 in endosomes following aqueous

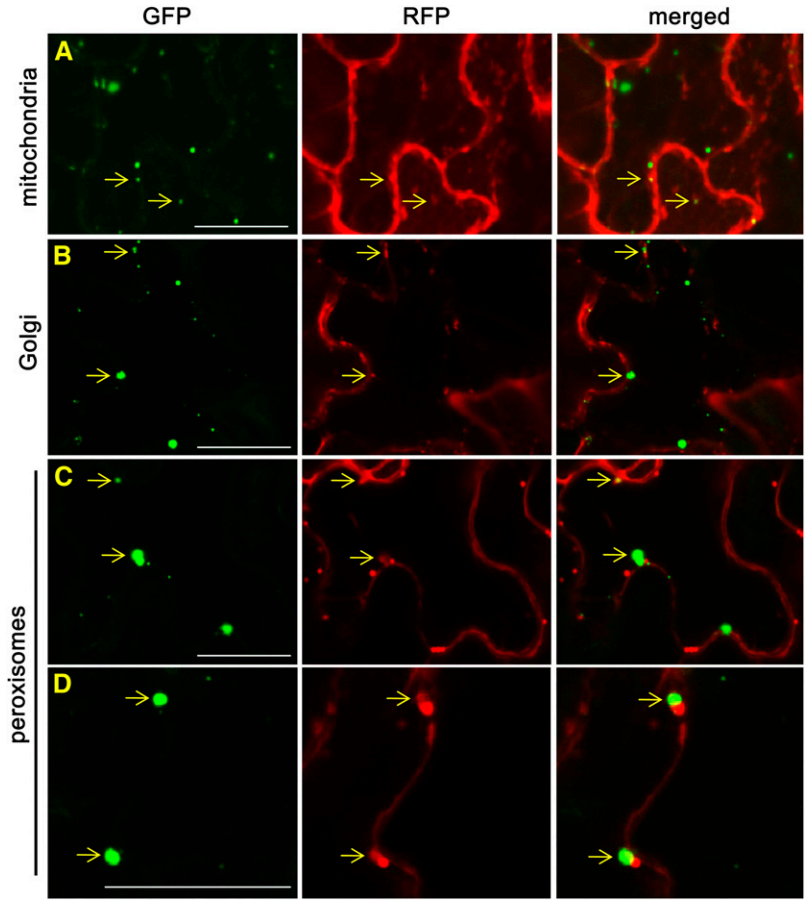

Figure 6. GFP-CRT1 Localizes in Endocytic Vesicle-Like Structures.

Confocal microscopy of *N. benthamiana* leaves transiently overexpressing *GFP-CRT1* together with red florescent protein (RFP; mCherry)-tagged markers for mitochondria (**[A]**; yeast cytochrome oxidase subunit IV), the Golgi complex (**[B]**; soybean α-1,2-mannosidase I), or peroxisomes (**[C]** and **[D]**; peroxisome targeting sequence 1; **[D]** is a higher magnification from an independent experiment). GFP is shown in green, while mCherry is in red (RFP); merged images of both are shown in yellow. Arrows identify sites where CRT1 and markers overlap. Bars = 20 μm.

two-phase separation but discounted it as a technical limitation. However, using marker antibodies to monitor the efficacy of the aqueous two-phase purification process, we conclude that localization of RPM1 in endosomes is legitimate (Figure 7).

Genome-Wide Transcriptome Analyses Revealed Altered Expression of Several *R* Gene–Dependent Genes in *crt1-2 crh1-1*

R gene–mediated resistance is accompanied by significant changes in the transcriptome (Tao et al., 2003; Sato et al., 2006). However, prior analysis of TCV-inoculated *crt1* mutant and wild-type plants failed to uncover any differences in the expression of a limited set of defense-related genes (Kang et al., 2008). To extend this study, the ATH1 GeneChip, which assesses expression of 23,288 genes, was used to monitor the *crt1-2 crh1-1* transcriptome in response to avirulent *Pst AvrRpt2* infection. RNAs from wild-type or *crt1-2 crh1-1* plants treated for 6 h with either buffer (W_m or M_m, respectively) or *Pst AvrRpt2* (W_p or M_p, respectively), as well as untreated wild-type and *crt1-2 crh1-1* plants (W_n or M_n, respectively), were used for expression analysis. Sixty-five genes that satisfied the following requirements were selected and designated *CRT1 Associated* (*CRA*) genes (Table 1): (1) statistically significant difference (q value < 0.05) in relative expression between W_p and M_p, and (2) statistically significant (q value < 0.05) and relatively large difference (fourfold change or higher) in relative expression between (M_p ÷ M_m) and (W_p ÷ W_m). Fold changes on a $\log_2$ scale based on calculation of W_p ÷ W_m were negative for most of the *CRA* genes (51 out of 65; see column A in Table 1), suggesting that expression of the *CRA* genes was mostly suppressed in wild-type plants following infection with *Pst AvrRpt2*. Interestingly, this suppression was largely compromised in *crt1-2 crh1-1* since the fold changes of these CRA genes in *crt1-2 crh1-1* [column B in Table 1; $\log_2$(M_p ÷ M_m)] were bigger than those in the wild type. This trend is better shown in the column B/A, which denotes the value of [(M_p ÷ M_m) ÷ (W_p ÷ W_m)] on a $\log_2$ scale, termed Δ*crt1-2 crh1-1*/WT.

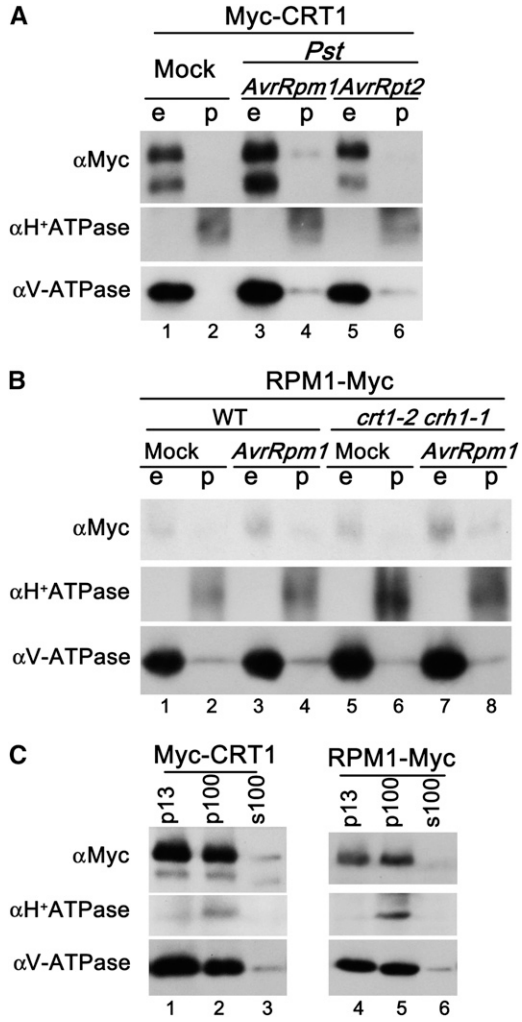

Figure 7. RPM1 and CRT1 Are Predominantly Localized to Endosomes.

(A) and **(B)** Aqueous two-phase separation of membranes prepared from transgenic *Arabidopsis* expressing *Myc-CRT1* **(A)** or *RPM1-Myc* **(B)**. Plasma membrane (p) and endomembrane (e) fractions were subjected to 6% SDS-PAGE (12% for αV-ATPase) followed by IB with the indicated antibodies; 10^6 cfu/mL of *Pst AvrRpm1* or *Pst AvrRpt2* was infected for 12 h.

(C) Two-step differential centrifugation of leaf extracts prepared from *Arabidopsis Myc-CRT1* or *RPM1-Myc* transgenic plants followed by IB using the indicated antibodies, as described in **(A)**. The extracts were centrifuged at 500*g* to remove any debris; the 500*g* supernatant was then sequentially centrifuged at 13,000*g* and 100,000*g* to generate low- (p13) and high-speed (p100) pellet fractions and the remaining supernatant (s100) fraction.

(A) to **(C)** At least three independent experiments were performed with similar results.

Based on The Arabidopsis Information Resource (TAIR) database annotation, the 65 *CRA* genes were categorized according to their known or deduced biological process and cellular location. *CRA* genes were overrepresented in several categories, based on the expected rate in the total 23,288 genes on the ATH1 chip (Figures 8A and 8B). Since a majority of the *CRA* genes displayed differential expression in response to avirulent *Pst* (Table 1, column A), these genes are overrepresented in the category termed "(a)biotic stress related." *CRA* genes also were significantly overrepresented in the categories encompassing "transport" and "other biological process" (Figure 8A). Statistical analysis of the cellular component categories revealed that the *CRA* genes were significantly overrepresented in the "endomembrane system," "cell wall/extracellular," "other cellular components," and "other membrane" categories (Figure 8B). Note that in our categories, the endomembrane system, also known as endosomes, includes the endoplasmic reticulum, Golgi complex, and vacuole.

To further identify those *CRA* genes whose expression pattern is altered in response to pathogen infection, rather than due to mock inoculation or differences between wild-type and *crt1-2 crh1-1* plants prior to infection, a heat map was drawn based on comparisons between the following four combinations: (1) W_m versus W_n, (2) M_m versus M_n, (3) W_m versus M_m, and (4) W_n versus M_n (see Supplemental Figure 7 online). Analysis of gene expression in mock versus untreated wild-type and *crt1-2 crh1-1* plants (1 and 2) revealed that a significant number of *CRA* genes respond to mock treatment. In addition, some *CRA* genes showed differences between wild-type versus mutant plants that received either a mock inoculation or no treatment (3 and 4), suggesting preexisting differences in their expression levels. To focus on genes whose expression differences between wild-type and *crt1-2 crh1-1* plants were associated with *R* gene–mediated defense, we selected 14 *CRA* genes that exhibited twofold or less difference in expression levels in all four comparisons (1 to 4; see Supplemental Table 1 online). Note that all of the raw numbers for Table 1 and Supplemental Figure 7 online are shown in Supplemental Table 1 online.

The influence of the CRT1 family on *R* gene–mediated responses was then assessed by monitoring the expression of these 14 *CRA* genes using real-time quantitative RT-PCR (qRT-PCR) analysis in wild-type and *crt1-2 crh1-1* plants; for comparison, the susceptible *rps2* also was included (left half of the panels in Figure 9; see Supplemental Figure 8 online). This analysis revealed that all 14 *CRA* genes displayed the same trends as observed in the ATH1 GeneChip analysis (cf. left half of the panels in Figure 9 and Supplemental Figure 8 online with Supplemental Table 1 online). Furthermore, this analysis revealed that the expression of seven of these 14 genes differed between the wild type and the *crt1-2 crh1-1* and *rps2* mutants following *Pst AvrRpt2* infection (left half of the panels in Figure 9). For instance, the expression of *CRA1*, *2*, and *3* was significantly induced in wild-type plants following *Pst AvrRpt2* infection, but this induction was largely missing in *rps2* plants and was significantly compromised in *crt1-2 crh1-1* plants (left half of the panels in Figures 9A to 9C). By contrast, the expression of *CRA4-7* was suppressed in wild-type plants following *Pst AvrRpt2* infection, but this suppression was largely compromised in *crt1-2 crh1-1* and *rps2* plants (left half of the panels in Figures 9D to 9G).

To assess expression of the *CRA* genes mediated by another *R* gene, the same 14 *CRA* genes were analyzed in wild-type, *crt1-2 crh1-1*, and *rpm1* plants in response to inoculation by *Pst*

Table 1. *CRA* Genes Identified in the ATH1 Chip Experiments

Locus	Annotation	B/A	A	B
At4g16590	CSLA1 (cellulose synthase-like A1)	**4.46**	−5.16	−0.70
At4g21680	Proton-dependent oligopeptide transport family protein	**4.43**	**0.24**	**4.67**
At5g24420	Glucosamine/galactosamine-6-phosphate isomerase-related	**3.43**	−2.40	**1.03**
At1g73480	α/β-Fold hydrolase	**3.15**	**0.81**	**3.96**
At5g62360	Invertase/pectin methylesterase inhibitor family protein	**3.05**	−4.66	−1.61
At1g20450	ERD10/LTI45 (early responsive to dehydration 10)	**2.81**	−2.78	**0.03**
At3g54820	PIP2;5 (plasma membrane intrinsic protein 2;5)	**2.76**	−3.89	−1.13
At5g24770; At5g24780	VSP2 (vegetative storage protein 2); VSP1	**2.75**	−3.70	−0.95
At3g45060	NRT2.6 (high affinity nitrate transporter 2.6)	**2.69**	−0.74	**1.95**
At3g04010	Glycosyl hydrolase family 17 protein	**2.68**	−0.48	**2.20**
At5g39580	Putative peroxidase	**2.65**	**0.20**	**2.85**
At5g52320	CYP96A4	**2.54**	−4.07	−1.52
At4g15210	β-Amylase 5	**2.52**	−2.85	−0.33
At4g01080	Unknown protein	**2.51**	−5.24	−2.73
At1g16850	Unknown protein	**2.49**	−2.94	−0.44
At4g35060	Heavy metal–associated domain-containing protein	**2.48**	−2.38	**0.10**
At5g40540	Putative protein kinase	**2.47**	−0.66	**1.81**
At1g04040	Acid phosphatase class B family protein	**2.47**	−4.22	−1.76
At1g04220	Putative β-ketoacyl-CoA synthase	**2.44**	−3.91	−1.47
At5g52310	COR78 (cold regulated 78)	**2.42**	−2.32	**0.11**
At3g12700	Aspartyl protease family protein	**2.42**	−1.41	**1.01**
At1g02400	GA2OX6/DTA1 (gibberellin 2-oxidase 6)	**2.39**	**1.15**	**3.53**
At2g22170 (CRA5)	Lipid-associated family protein	**2.38**	−3.66	−1.28
At5g13930	CHS (chalcone synthase)	**2.35**	−4.82	−2.48
At3g50970	LTI30 (low temperature induced 30)	**2.34**	−1.51	**0.84**
At2g30540	Glutaredoxin family protein; PAO2 (polyamine oxidase 2)	**2.34**	−1.78	**0.56**
At3g11480	BSMT1; *S*-adenosylmethionine-dependent methyltransferase	**2.32**	−1.88	**0.44**
At4g36360	BGAL3 (β-galactosidase 3)	**2.31**	−3.77	−1.46
At3g06035	Uncharacterized GPI-anchored protein	**2.29**	−3.60	−1.31
At3g05640	Putative protein phosphatase 2C	**2.28**	−2.62	−0.34
At1g66760	MATE efflux family protein	**2.26**	−0.78	**1.48**
At1g26770	EXPA10 (expansin A10)	**2.26**	−2.61	−0.35
At1g05680	UDP-glucoronosyl/UDP-glucosyl transferase family protein	**2.23**	−0.78	**1.45**
At2g42530 (CRA12)	COR15B	**2.22**	−2.48	−0.26
At2g36870 (CRA6)	Xyloglucan:xyloglucosyl transferase, putative	**2.22**	−4.44	−2.22
At5g37300	Unknown protein	**2.21**	−3.61	−1.40
At5g47240	NUDT8 (Nudix hydrolase homolog 8)	**2.21**	−2.67	−0.46
At1g20440	COR47 (cold regulated 47)	**2.21**	−2.07	**0.13**
At5g01340	Mitochondrial substrate carrier family protein	**2.21**	−0.08	**2.12**
At3g14395	Unknown protein	**2.17**	−6.00	−3.84
At1g55260 (CRA4)	Lipid binding	**2.17**	−4.56	−2.39
At4g04840	Met sulfoxide reductase domain-containing protein	**2.16**	−3.07	−0.92
At3g48460	GDSL-motif lipase/hydrolase family protein	**2.13**	−3.27	−1.14
At5g54300	Unknown protein	**2.09**	−2.88	−0.79
At5g61810 (CRA7)	Mitochondrial substrate carrier family protein	**2.08**	−2.97	−0.88
At1g52030; At1g52040	MBP2 (myrosinase binding protein 2); MBP1	**2.08**	−1.58	**0.50**
At3g57010	Strictosidine synthase family protein	**2.07**	−2.18	−0.12
At3g23920 (CRA13)	β-Amylase 1	**2.05**	−2.04	**0.01**
At4g29020	Gly-rich protein	**2.05**	−1.67	**0.38**
At3g54400 (CRA14)	Aspartyl protease family protein	**2.02**	−3.57	−1.54
At2g43018 (CRA8); At2g43020 (CRA9)	CPuORF17 (conserved peptide upstream open reading frame 17)	**2.02**	−1.35	**0.68**
At2g36590	ProT3 (Pro transporter 3)	**2.02**	−2.92	−0.90
At1g26390 (CRA1)	FAD binding domain-containing protein	−2.00	**5.73**	**3.72**
At2g45510 (CRA11); At2g44890 (CRA10)	CYP704A2; CYP704A1	−2.03	**0.62**	−1.42
At1g49470 (CRA3)	Unknown protein	−2.09	**1.28**	−0.81
At2g04070 (CRA2)	MATE efflux family protein	−2.11	**5.18**	**3.06**
At3g49340	Cys proteinase, putative	−2.34	**0.09**	−2.25
At3g61210	Embryo-abundant protein-related	−2.35	**0.22**	−2.14

(Continued)

Table 1. (continued).

Locus	Annotation	B/A	A	B
At4g25100	FSD1 (FE superoxide dismutase 1), iron superoxide dismutase	−2.56	**1.47**	−1.09
At4g14020	Rapid alkalinization factor (RALF) family protein	−2.73	**1.37**	−1.36
At1g76960	Unknown protein	−3.03	**2.49**	−0.54

Relative RNA expression value is designated as W_m for the wild type and M_m for *crt1-2 crh1-1* with mock, as W_p for the wild type and M_p for the mutant with *Pst AvrRpt2*, and as W_n for the wild type and M_n for the mutant that received no treatment. Fold changes on a $\log_2$ scale are presented based on calculation of W_p ÷ W_m (column A), M_p ÷ M_m (column B), and (M_p ÷ M_m) ÷ (W_p ÷ W_m) (column B/A). Genes displaying a significantly different expression values ($q < 0.05$) between W_p and M_p and between W_p ÷ W_m and M_p ÷ M_m ($q < 0.05$; fourfold change or higher when higher value was divided by lower value) were selected. Rows with multiple loci indicate that the probe analyzes RNA from indicated loci. Genes selected for qRT-PCR and positive numeric values are highlighted in bold.

AvrRpm1 (right half of the panels in Figure 9; see Supplemental Figure 8 online). Similar to the *RPS2*-mediated responses shown above, expression of *CRA1-3* was induced and *CRA4-7* was suppressed in *Pst AvrRpm1*–inoculated wild-type plants, suggesting that expression patterns of *CRA1-7* mediated by RPM1 and RPS2 are comparable. In comparison, the RPM1-mediated induction/suppression of these genes was compromised in *crt1-2 crh1-1* to various degrees (right half of the panels in Figure 9). Together, these results suggest that full *R* gene–dependent induction/suppression of the *CRA1-7* genes in response to *Pst AvrRpt2* or *Pst AvrRpm1* requires the CRT1 family.

DISCUSSION

Here, we show that CRT1 is involved in *R* gene–mediated resistance to bacterial and oomycete pathogens, in addition to its previously reported role in resistance to TCV (Kang et al., 2008). Consistent with this finding, CRT1 interacts with a wide range of R proteins, including those from the two major groups, CC-NB-LRR and TIR-NB-LRR. CRT1's role in *R* gene–mediated resistance does not appear to be limited to *Arabidopsis*, since VIGS of an *N. benthamiana* CRT1 homolog(s) compromised HR mediated by Pto and RPM1. Furthermore, CRT1 homologs have

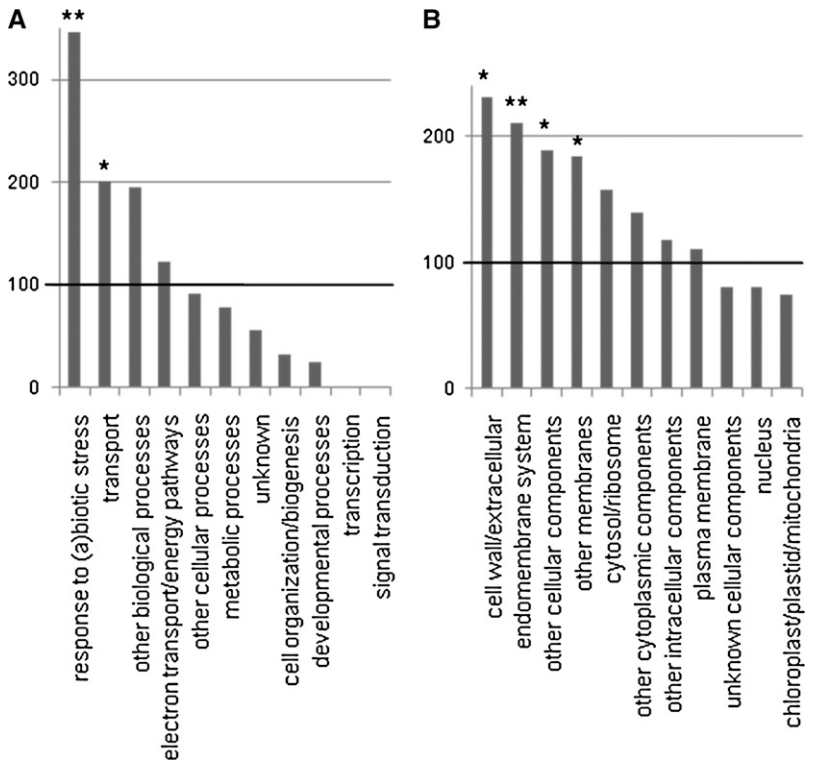

Figure 8. Degree of Representation of *CRA* Genes in the Biological Process and Cellular Component Categories Based on Annotation in the TAIR Database.

Biological process **(A)**; cellular component **(B)** categories. The degree of representation in percentage was calculated relative to the representation of all the genes on the Affymetrix ATH1 array with 100 indicating that there is no over- or underrepresentation. Statistical significance was determined using a one-sample χ^2 test: *$P < 0.05$; **$P < 0.01$.

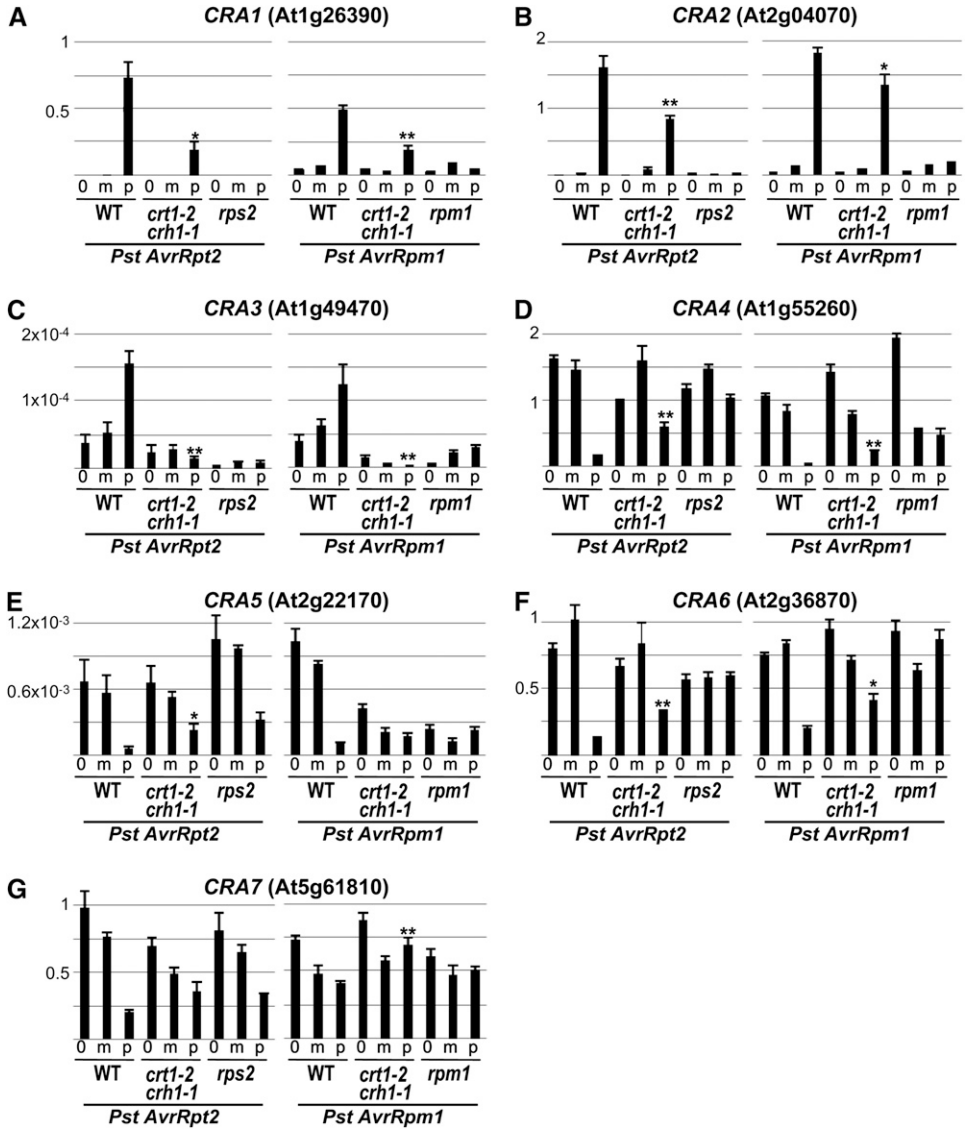

Figure 9. Expression of *CRA* Genes after Infection by *Pst AvrRpt2* or *Pst AvrRpm1*.

Real-time qRT-PCR was performed on RNA from 4-week-old wild-type, *crt1-2 crh1-1*, *rps2*, or *rpm1* plants. Leaves that were infected with 10^6 cfu/mL of *Pst AvrRpt2* or *Pst AvrRpm1* (p) or mock (m) were harvested at 6 h after infection; untreated control leaves were harvested at 0 DAI (0). The *y* axis shows relative expression levels of the indicated gene compared with the *TIP41-like* gene (Czechowski et al., 2005). The mean ± SE (n = 4 for *Pst AvrRpt2* and n = 6 for *Pst AvrRpm1*) is presented. Statistical difference between the wild type and *crt1-2 crh1-1* infected with *Pst AvrRpt2* or *Pst AvrRpm1* is indicated; *P < 0.05; **P < 0.01 (*t* test).

been identified in all plant species whose genomes have been sequenced. Since pathogen-induced Ca^{2+} elevation was compromised in *crt1-2 crh1-1* plants, whereas the HR triggered by Nt MEK2^{DD} was unaffected in *CRT1*-silenced *N. benthamiana*, CRT1 appears to function at a very early step in the defense signaling pathway(s).

CRT1 was previously shown to belong to the GHKL ATPase/Kinase superfamily (Kang et al., 2008). One of the founding members of this superfamily is HSP90, a well-known chaperone that interacts with R proteins. Although CRT1 and HSP90 share homology limited to the ATPase domain, CRT1 may function as a cochaperone with HSP90. Consistent with this possibility, CRT1 physically associated with HSP90 in the co-IP assay (Figure 1B). However, CRT1 did not associate with the HSP90-interacting proteins RAR1 and SGT1 (Figure 1B). Further suggesting that CRT1 is not a component of an HSP90-RAR1-SGT1-R protein complex is the observation that HSP90 and RAR1 are primarily localized in the cytosol and nucleus (Pratt and Toft, 2003; Wang et al., 2008), whereas CRT1 resides in endosomes (Figures 6 and 7). In addition, loss of functional HSP90, RAR1, or SGT1 leads to

significantly lower R protein accumulation (Holt et al., 2005; Azevedo et al., 2006; Hubert et al., 2009), but little change was observed in the stability of RPM1 in *crt1-2 crh1-1* plants (see Supplemental Figure 3 online).

Based on co-IP analysis, CRT1 appears to interact only with R proteins in their inactive state; indeed, CRT1 failed to interact with any of the autoactivated R proteins tested, including ssi4, RPM1, RPS2, and RCY1. This finding, combined with the demonstration that plants exhibiting reduced expression of functional CRT1 family members are compromised for disease resistance or HR formation, suggests that CRT1 is involved in activating R proteins. Two mechanisms (that are not mutually exclusive) could be invoked to explain this putative function of CRT1. In the first, CRT1 may be required for formation of an activation-competent R protein complex (Figure 10A). R proteins interact with multiple proteins prior to activation, including guardee (which may actually be a decoy or recognition factor in some cases; van der Hoorn and Kamoun, 2008; Collier and Moffett, 2009), and (co)chaperones such as HSP90 and RAR1. Thus, CRT1 might function as a scaffold protein that helps gather all of the necessary components for forming an activation-competent R protein complex. However, a yeast two-hybrid screen searching for CRT1-interacting proteins did not identify any known host guardee proteins (H.-G. Kang and D.F. Klessig, unpublished data), arguing against this possibility. This result is not definitive, given the large number of scaffold proteins crucial in animal immune responses (Shaw and Filbert, 2009) and the possibility that a scaffold protein need not interact directly with a guardee, which would preclude its identification in a yeast two-hybrid screen.

Alternatively, CRT1 may play a role in R protein activation (Figure 10B). Changes in inter- and intramolecular interactions have been reported in several R proteins following activation (Bent and Mackey, 2007; Rairdan and Moffett, 2007; Rairdan et al., 2008). The NB domain and its neighboring domain, ARC (APAF-1, R protein, and CED-4), of R proteins (termed the NB-ARC domain) have ATPase activity and likely function as part of a switch for conformational changes that lead to activation (Tameling et al., 2002, 2006; Leipe et al., 2004). Indeed, several autoactive R proteins carry mutations in the NB-ARC domain (Bendahmane et al., 2002; Shirano et al., 2002; Tameling et al., 2006). Moreover, the NACHT domain of animal NLR proteins, which is the counterpart of the NB-ARC unit, is responsible for ATP-dependent oligomerization leading to apoptosis (reviewed in Martinon et al., 2009). In this context, it is intriguing that, unlike other factors, CRT1 interacts with the NB-ARC domain of an R protein in planta (Kang et al., 2008). Thus, it is tempting to speculate that CRT1's ATPase activity is involved in (i) converting the inactive R protein to its activation-competent form, (ii) converting the activation-competent R protein to its active form once an activation cue is present, and/or (iii) mediating transmission of the activation signal to a downstream component(s) (Figure 10B). Consistent with this model, the *crt1* mutant, which encodes a prematurely truncated protein lacking the ATPase domain, was originally identified in our genetic screen by the loss of HRT-mediated cell death; *crt1* plants also display reduced resistance to TCV infection (Kang et al., 2008). Interestingly, several truncated CRT1 mutants lacking the ATPase domain display dominant-negative suppression of cell death triggered by the autoactivated ssi4 R proteins (Kang et al., 2008). Since ssi4 contains a mutation that shifts it to a constitutively active state, this result suggests that R protein activation is a multistep process that requires other modifications to occur prior to, or in conjunction with, the ATPase function of CRT1. Given that the guardee proteins (alternatively designated recognition factors or bait proteins) and the Arc2 subdomain of R proteins likely have multiple functions in modulating R protein activity (Collier and Moffett, 2009), it would not be surprising if CRT1 also served multiple functions in R protein activation.

The endomembrane system, which is essential for trafficking proteins, metabolites, and other molecules, generally comprises the endoplasmic reticulum, the Golgi complex, vacuoles, and endosomes (Surpin and Raikhel, 2004). Growing evidence indicates that metabolite transport is an essential part of plant defense responses, including deposition of lignin and callose at the site of pathogen challenge (Field et al., 2006). Moreover, two SNARE proteins, which are implicated in vesicle trafficking, play roles in basal and nonhost resistance in *Arabidopsis* and barley (*Hordeum vulgare*; PEN1 and ROR2, respectively; Collins et al., 2003). Syp132, another SNARE protein, contributes not only to basal resistance but also to *R* gene–mediated resistance (Kalde et al., 2007), suggesting broad participation of the trafficking system in plant defense. Since CRT1 is an endosome-localized protein, it may regulate resistance by playing a role in this trafficking-related defense. Indeed, endomembrane system-related genes are significantly overrepresented in the *CRA* genes identified from the ATH1 chip analyses, as are genes from the "transport" category (Figure 8). For example, CRA2 is a MATE transporter, which was previously identified as *Arabidopsis* DTX1 (detoxification 1) and shown to complement an *Escherichia coli* mutant defective in multidrug resistance (Li et al., 2002). Its expression was highly induced in wild-type plants by *RPS2*-dependent recognition of *Pst AvrRpt2* (Figure 9B) but was compromised in *crt1-2 crh1-1*. EDS5, an essential component of salicylic acid–dependent signaling, also belongs to this MATE transporter family. *EDS5* was also rapidly and highly induced by *Pst AvrRpt2* (Nawrath et al., 2002). *EDS5* expression, however, was not altered in *crt1-2 crh1-1* (26-fold induction by *Pst AvrRpt2* over mock in both the wild type and *crt1-2 crh1-1*), suggesting that these two MATE transporters likely function independently.

Recent developments provide some clues as to what types of metabolites might be involved in the resistance-associated trafficking in which CRT1 appears to participate. Based on microarray analysis, NPR1, a crucial regulator of salicylic acid–mediated resistance, controls the expression of protein secretory pathway genes involved in the secretion of pathogenesis-related proteins (Wang et al., 2005). PEN2, which is localized to mobile endosomes, is involved in metabolizing a glucosinolate to a breakdown product that is a crucial signaling molecule for a broad spectrum of defense responses (Bednarek et al., 2009; Clay et al., 2009). In addition, R proteins, including MLA and N, are differentially localized upon activation (Burch-Smith et al., 2007; Shen et al., 2007). Some R proteins, including RPP1A (Weaver et al., 2006), RPS4 (Weaver et al., 2006; Wirthmueller et al., 2007), and RPM1 (Figure 7B), have been localized to endosomes. Interestingly, the

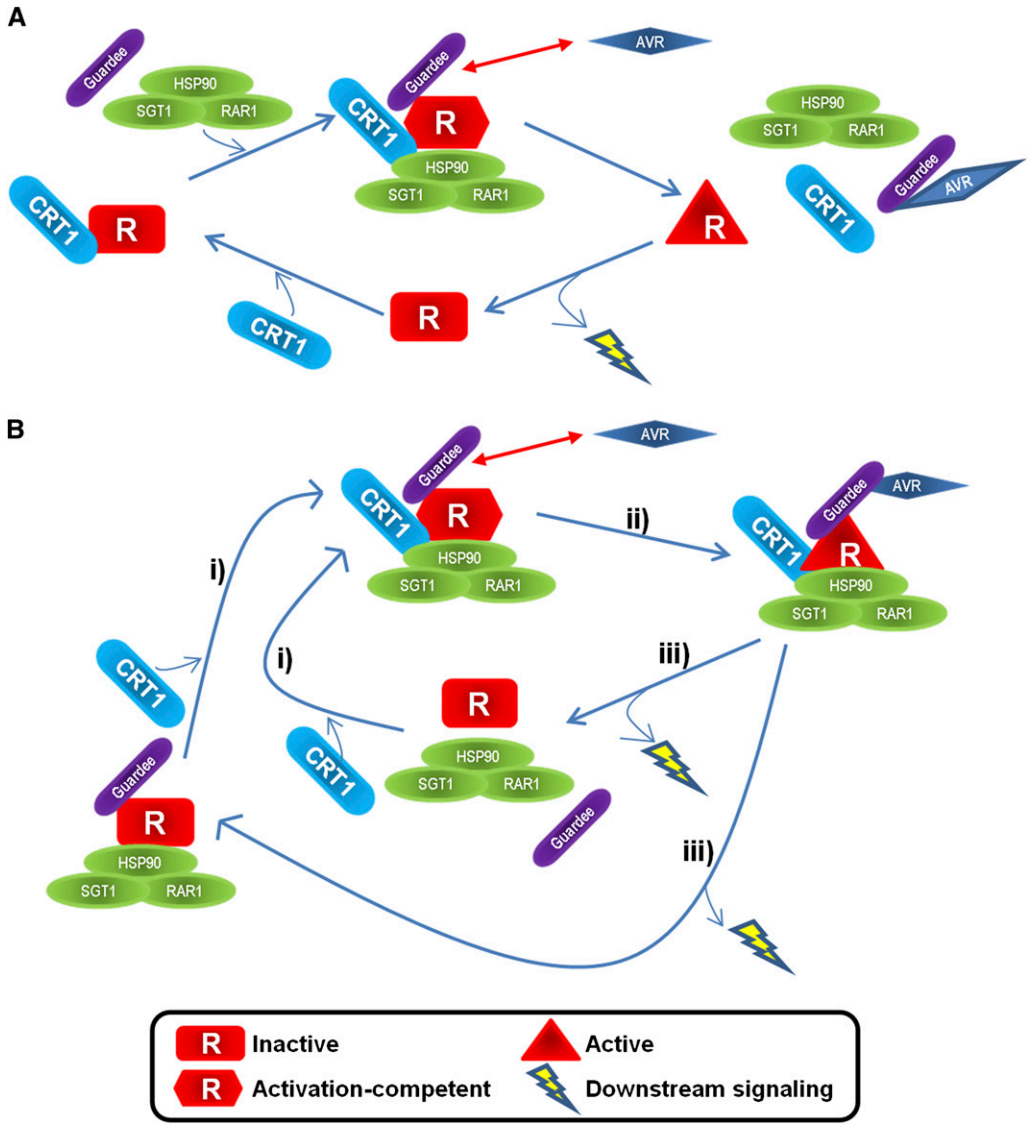

Figure 10. Model of CRT1's Putative Function(s) in R Protein–Mediated Defense Signaling.

(A) CRT1 may functions as a scaffold protein that helps gather all of the necessary components for forming an activation-competent R protein (represented as a red hexagon) complex, including guardee and cochaperones (HSP90, RAR1, and SGT1). Subsequent interaction with pathogen-derived avirulent factor (AVR) would trigger downstream signaling.

(B) CRT1 might play an active role in three potential energy-dependent processes using its ATPase activity to either (i) convert the inactive R protein to its activation-competent form, (ii) convert the activation-competent R protein to its active form once an activation cue (e.g., AVR) is present, or (iii) mediate transmission of the activation signal to a downstream component(s).

animal PAMP receptors, TLR9 and TLR4, which play important roles in modulating innate and adaptive immunity, require localization to endosomes for their functions (Honda et al., 2005; Husebye et al., 2006). Based on the many similarities between innate immunity in animals and plants, we suggest that a population of plant R proteins resides in endosomes where, following pathogen attack, CRT1 performs a critical function required for their activation as proposed in Figure 10. Once activated, R proteins may relocate to other subcellular compartments with the concomitant disruption of CRT1–R protein interaction.

In summary, CRT1 physically associates with a wide range of R proteins (and with the chaperone HSP90), and it is required for full resistance to the viral, bacterial, and oomycete pathogens recognized by these R proteins. Strikingly, activation of these R proteins appears to disrupt the CRT1–R protein interaction. Together, these results, along with the requirement of CRT1 for increases in cytosolic Ca^{2+} levels and the ability of *CRT1*-silenced *N. benthamiana* to develop Nt $MEK2^{DD}$–induced cell death, argue that CRT1 plays a crucial role early in *R* gene–mediated defense signaling. The endosomal location

of CRT1 and RPM1, as well as the large number of *CRA* genes associated with the endomembrane system, further suggest that this subcellular compartment is crucial for plant defense responses.

METHODS

DNA Constructs and Phylogenetic Analysis

Plant overexpression constructs for *Myc-CRT1*, *GFP-HA*, *HRT-HA*, *HRTΔLRR-HA*, *RPS2m-HA* (Kang et al., 2008), *GFP-Flag*, *TCV*, *mTCV* (Bhattacharjee et al., 2009), *Pto*, *AvrPto*, *AvrPtoB*$_{1-387}$ (Abramovitch et al., 2006), and *AvrB* (Ong and Innes, 2006) were described previously. *RCY1-HA*, *rcy1-3-HA*, *rcy1-6-HA RPP8-HA*, *RPP8c-HA*, *RPM1ΔC-HA* (1 to 734 amino acids), *SNC1-HA*, *Pto-HA*, *GFP-CRT1*, Nt *MEK2*^{DD} (Yang et al., 2001), and *Aequorin* were cloned into *Xho*I and *Spe*I sites of pER8 (Zuo et al., 2000) for overexpression in plants. Note that *Aequorin* was PCR amplified from pMAQ carrying the *Aequorin* gene from *Aequorea victoria* (Knight et al., 1991). Nb *HSP90* (GQ845021), Nt *Rar1* (Liu et al., 2002b), and Nb *SGT1* (Leister et al., 2005) were cloned into *Bam*HI and *Xba*I sites of pBin61 carrying HA tag in 3′ end (Sacco et al., 2007) for overexpression in plants. For protoplast transfection, *GFP-HA*, *Myc-CRT1*, *HRTΔLRR* (1 to 513 amino acids)-*HA*, and *Pto-HA* were cloned into pJD301 (Anderson et al., 2006). For VIGS, Nb *CRT1* (GQ855284) amplified from *N. benthamiana* cDNA was cloned into the pTRV2 vector for TRV-based VIGS in *N. benthamiana*, as described (Liu et al., 2002a). All the primers used in RT-PCR are listed in Supplemental Table 2 online. Multiple sequence alignments were produced using ClustalW (with default parameters in MEGA4.1) and are provided in Supplemental Data Set 1 online. Phylogenetic analysis was performed using MEGA 4.1 with the UPGMA method (Tamura et al., 2007). The tree is drawn to scale and midpoint rooted, with branch lengths in the same units as those of the evolutionary distances used to infer the phylogenetic tree. Bootstrap values calculated from 2000 replicates are shown.

Tomato Protoplast Transfection, VIGS, *Agrobacterium tumefaciens*–Mediated Transient Expression in *Nicotiana benthamiana*, and Generation of Transgenic *Arabidopsis*

Protoplasts prepared from 4-week-old tomato (*Solanum lycopersicum*) *prf3* or its wild-type Rio Grande parent were transfected as described (Xiao et al., 2007). VIGS in *N. benthamiana* and a cell death assay were performed as described (del Pozo et al., 2004). *Agrobacterium*-mediated transient expression in *N. benthamiana* was performed as described (Kang et al., 2008). Estradiol-inducible pER8-Myc-CRT1 were transformed into *A. tumefaciens* strain GV3101 carrying the plasmid MP90. The *crt1-2 crh1*-1 mutant was then used as recipient for *Agrobacterium*-mediated transformation (Bechtold et al., 1993).

Co-IP and IB Analyses

Co-IP and IB were performed as described (Kang et al., 2008). Equal loading of proteins was checked by staining the polyvinylidene fluoride membrane (Millipore) with Coomassie Brilliant Blue to visualize the large subunit of RuBPCase. αH$^+$ATPase and αV-ATPase marker antibodies were purchased from Agrisera.

Two-Step Differential Centrifugation and Aqueous Two-Phase Separation

Two-step differential centrifugation and extraction of *Arabidopsis thaliana* membranes were performed as described (Darsow et al., 1997; Wirthmueller et al., 2007), with the following modifications: ~2 g of *Arabidopsis* leaves were homogenized in 10 mL of the described buffer at 4°C without a freeze-thaw using a T10 Ultra-Turrax homogenizer (IKA).

Pathogen Infection, Generation of Transgenic *Arabidopsis*, Measurement of [Ca^{2+}] by Aequorin Luminometry, Confocal Microscope Imaging, and Trypan Blue Staining

Infection with *Pst* (Kang et al., 2008) or *Hyaloperonospora arabidopsidis* (Menke et al., 2004) was performed as described. *Arabidopsis* transformation was performed as described (Kang et al., 2008). Measurement of [Ca^{2+}] by Aequorin luminometry was performed as described (Grant et al., 2000) with the following alterations: 3 d before the measurement, 3-week-old *Arabidopsis* was treated with 30 μM estradiol to induce *Aequorin* gene expression. Upon *Pst* or mock infection, luminescence counts were integrated every 10 s over a 210-min period on a luminometer (9200-102; Turner Biosystems).

Confocal images were collected on a Leica TCS-SP5 confocal microscope. GFP was excited with an argon laser (488 nm), and emitted light was collected between 500 and 520 nm. mCherry was excited with a HeNe laser (594 nm), and emitted light was collected from 600 to 620 nm. Sequential scanning was used to avoid bleed-through. Images were processed using Leica LAS-AF software (version 1.8.2). Trypan blue staining was performed as described (Bowling et al., 1994).

RNA Extraction, RT-PCR, and Microarray Experiments

RNA extraction was performed using the RNeasy plant mini kit (Qiagen). cDNA was generated by the SuperScript III kit (Invitrogen). RT-PCR was performed as described (Kang et al., 2008) except that SYBR green staining solution (Sigma-Aldrich) was used for DNA visualization. Real-time qRT-PCR was performed using SYBR Green qPCR mix as suggested by the manufacturer (Invitrogen) with the primers listed in Supplemental Table 2 online on an ABI PRISM 7900HT. Each of two biological replicates was analyzed in duplicate. Relative expression level was calculated from the difference between threshold cycle (Ct) values of reference and target genes (Schmittgen and Livak, 2008). The reference gene is *TIP41-like* (AT4G34270; Czechowski et al., 2005).

Affymetrix ATH1 microarrays were used for transcriptome analyses (Redman et al., 2004). Transcriptome analyses included the wild type and *crt1-2 crh1-1*, involving three biological repeats. The data are available from Array-Express. Labeling, hybridization to arrays, and scanning were performed at the Cornell Microarray Facility (Ithaca, NY) as described (Han et al., 2007). ATH1 data generated in this work were normalized using RMA Expression (Irizarry et al., 2003).

Microarray Data Preprocessing

Samples from mock- and *Pst AvrRpt2*-treated plants (W_m, M_m, W_p, and M_p) and the mock-treated samples and no treatment plants (W_m, M_m, W_n and M_n) were processed separately due to the experimental design. The raw microarray data (CEL files) were preprocessed using GC-RMA (Wu et al., 2004) after quality control using the affyPLM package from Bioconductor (http://www.bioconductor.org/). GC-RMA gives a bimodal distribution of $\log_2$ expression values. The values corresponding to the lower peak represent values that are mostly noise. Gene probes satisfying either of the following criteria were considered to have a true signal and were used for subsequent analyses: signal intensity in any sample is higher than 8 or signal intensities of all samples are above their valley values. The valley values were defined as follows: data from each array were equispaced 50 times (a class interval is 0.2 $\log_2$) to determine a class with the least frequency. A mean of the least frequent class interval was used as a valley value. Annotation of probes to Arabidopsis Genome Initiative loci was performed using affy_ATH1_array_elements-2008-5-29.txt in the TAIR database.

Microarray Data and Statistical Analysis

Selected probe sets were fitted to a linear model:

$$S_{ijkl} = P_i : G_j : T_k + R_l + \varepsilon_{ijkl}$$

where S is $\log_2$ signal intensity; P, G, T, and R are probe set, genotype, treatment, and replicate effects; ε is residual. $P:G:T$ is an interaction term. For the no pathogen treatment data set, no treatment (0 h) and mock inoculation were considered different treatments. The empirical Bayes method was used for variance shrinkage. The P values were corrected for multiple tests to obtain the q-values as described (Benjamini and Hochberg, 1995). The above procedure was performed using R and limma packages in Bioconductor. To evaluate enrichment in the Gene Ontology categories, known or deduced functions of the 65 *CRA* genes were annotated with TAIR9 as of June 2009. A one-sample χ^2 test was performed for each term using the chisq.test function with 10,000 Monte Carlo simulation replicates in R (http://www.R-project.org) to statistically evaluate significance of the enrichment. GO categories with P values < 0.05 in one-sided tests were considered significant.

Accession Numbers

Sequence information in this study can be found in GenBank or Sol Genomic Network (SGN) databases under the following accession numbers: Sl CRT1 (SGN-U349134), St CRT1 (SGN-U273098), Nb CRT1 (GQ855284), Cc CRT1 (SGN-U357963), Vv CRT1 (CAO48278), Os CRT1 (AAK70637), Pp CRT1 (XP_001762322), Zm CRT1 (ACG47873), Nb HSP90 (GQ845021), Nt RAR1 (AF480487; Liu et al., 2002b), and Nb SGT1 (AY899199; Leister et al., 2005). Germplasm identification numbers for the seeds in this study can be found in TAIR as follows: *crt1-2* (SAIL_893_B06), *crh1-1* (SALK_072774), and *crh2-1* (SALK_000009). Microarray data in this study have been deposited in the Array-Express database with the accession number NASCARRAYS-527.

Supplemental Data

The following materials are available in the online version of this article.

Supplemental Figure 1. Transient Expression of RPS2m and RPM1ΔC in *N. benthamiana* and Myc-CRT1 in Tomato Protoplasts.

Supplemental Figure 2. Characterization of the *crt1-2*, *crh1-1*, and *crt1-2 crh1-1* Mutants.

Supplemental Figure 3. Stability of RPM1 Is Unaffected in *crt1-2 crh1-1.*

Supplemental Figure 4. Disease Symptoms and Pathogen Growth after Infection with *H. arabidopsidis* Emco5.

Supplemental Figure 5. RT-PCR Analysis of *CRT1*-Silenced *N. benthamiana* Plants.

Supplemental Figure 6. Overexpression of *Myc-CRT1* Restores *RPM1*-Mediated Resistance in *crt1-2 crh1-1.*

Supplemental Figure 7. Heat Map Analysis of the *CRA* Genes with Respect to Mock and No Treatment Controls.

Supplemental Figure 8. Several *CRA* Genes Display Altered Gene Expression in *crt1-2 crh1-1* Compared with the Wild Type after *Pst AvrRpt2* or *Pst AvrRpm1* Infection.

Supplemental Table 1. List of *CRA* Genes with Raw Expression Levels.

Supplemental Table 2. Sequence of Oligonucleotides Used in RT-PCR Analysis.

Supplemental Data Set 1. Text File of the Alignment Used to Generate the Phylogenetic Tree Shown in Figure 3A.

Supplemental Movie 1. Cytoplasmic Streaming of the CRT1-GFP Fusion Protein and the mCherry-Tagged Peroxisome Marker.

ACKNOWLEDGMENTS

We thank D'Maris Dempsey for critical comments on the manuscript and Eun A Kim for technical support. We thank the following for providing critical biological reagents: Jeffery L. Dangl (*RPM1-Myc* line); Murray Grant (pMAQ); and Peter Moffett, Malanie Sacco, and Saikat Bhattacharjee (HSP90, RAR1, and SGT1 clones). We also thank the following for advice and for assistance: Mamta Srivastava and Sondra G. Lazarowitz (confocal microscopy), Jinwook Lee and Je Gun Joung (statistical analysis), Hanh Nguyen and Inhwa Yeam (generation of tomato protoplasts), Je Min Lee (real-time PCR analysis), Georg Jander (generation of *crt1-2 crh1-1*), Lennart Wirthmueller and Jane Parker (aqueous two-phase separation), and Chris Stefan (two-step differential centrifugation). This work was supported by grants from the National Science Foundation (IOB-0641576) to D.F.K. and P.K. and the U.S.–Israel Binational Agricultural Research and Development Fund (IS-4159-08C) to G.B.M.

Received September 26, 2009; revised February 10, 2010; accepted March 9, 2010; published March 23, 2010.

REFERENCES

Aarts, N., Metz, M., Holub, E., Staskawicz, B.J., Daniels, M.J., and Parker, J.E. (1998). Different requirements for EDS1 and NDR1 by disease resistance genes define at least two *R* gene-mediated signaling pathways in Arabidopsis. Proc. Natl. Acad. Sci. USA **95:** 10306–10311.

Abramovitch, R.B., Janjusevic, R., Stebbins, C.E., and Martin, G.B. (2006). Type III effector AvrPtoB requires intrinsic E3 ubiquitin ligase activity to suppress plant cell death and immunity. Proc. Natl. Acad. Sci. USA **103:** 2851–2856.

Abramovitch, R.B., Kim, Y.J., Chen, S., Dickman, M.B., and Martin, G.B. (2003). Pseudomonas type III effector AvrPtoB induces plant disease susceptibility by inhibition of host programmed cell death. EMBO J. **22:** 60–69.

Anderson, J.C., Pascuzzi, P.E., Xiao, F., Sessa, G., and Martin, G.B. (2006). Host-mediated phosphorylation of type III effector AvrPto promotes *Pseudomonas* virulence and avirulence in tomato. Plant Cell **18:** 502–514.

Axtell, M.J., and Staskawicz, B.J. (2003). Initiation of RPS2-specified disease resistance in Arabidopsis is coupled to the AvrRpt2-directed elimination of RIN4. Cell **112:** 369–377.

Azevedo, C., Betsuyaku, S., Peart, J., Takahashi, A., Noel, L., Sadanandom, A., Casais, C., Parker, J., and Shirasu, K. (2006). Role of SGT1 in resistance protein accumulation in plant immunity. EMBO J. **25:** 2007–2016.

Azevedo, C., Sadanandom, A., Kitagawa, K., Freialdenhoven, A., Shirasu, K., and Schulze-Lefert, P. (2002). The RAR1 interactor SGT1, an essential component of *R* gene-triggered disease resistance. Science **295:** 2073–2076.

Barth, C., and Jander, G. (2006). Arabidopsis myrosinases TGG1 and TGG2 have redundant function in glucosinolate breakdown and insect defense. Plant J. **46:** 549–562.

Bechtold, N., Ellis, J., and Pelletier, G. (1993). In planta Agrobacterium mediated gene transfer by infiltration of adult *Arabidopsis thaliana* plants. C. R. Acad. Sci. III. Sci. Vie **316:** 1194–1199.

Bednarek, P., Pislewska-Bednarek, M., Svatos, A., Schneider, B., Doubsky, J., Mansurova, M., Humphry, M., Consonni, C., Panstruga, R., Sanchez-Vallet, A., Molina, A., and Schulze-Lefert, P. (2009). A glucosinolate metabolism pathway in living plant cells mediates broad-spectrum antifungal defense. Science **323:** 101–106.

Belkhadir, Y., Subramaniam, R., and Dangl, J.L. (2004). Plant disease resistance protein signaling: NBS-LRR proteins and their partners. Curr. Opin. Plant Biol. **7:** 391–399.

Bendahmane, A., Farnham, G., Moffett, P., and Baulcombe, D.C. (2002). Constitutive gain-of-function mutants in a nucleotide binding site-leucine rich repeat protein encoded at the Rx locus of potato. Plant J. **32:** 195–204.

Benjamini, Y., and Hochberg, Y. (1995). Controlling the false discovery rate: A practical and powerful approach to multiple testing. J.R. Stat. Soc. **57:** 289–300.

Bent, A.F., and Mackey, D. (2007). Elicitors, effectors, and *R* genes: The new paradigm and a lifetime supply of questions. Annu. Rev. Phytopathol. **45:** 399–436.

Bhattacharjee, S., Zamora, A., Azhar, M.T., Sacco, M.A., Lambert, L.H., and Moffett, P. (2009). Virus resistance induced by NB-LRR proteins involves Argonaute4-dependent translational control. Plant J. **58:** 940–951.

Birch, P.R., Boevink, P.C., Gilroy, E.M., Hein, I., Pritchard, L., and Whisson, S.C. (2008). Oomycete RXLR effectors: Delivery, functional redundancy and durable disease resistance. Curr. Opin. Plant Biol. **11:** 373–379.

Block, A., Li, G., Fu, Z.Q., and Alfano, J.R. (2008). Phytopathogen type III effector weaponry and their plant targets. Curr. Opin. Plant Biol. **11:** 396–403.

Bowling, S.A., Guo, A., Cao, H., Gordon, A.S., Klessig, D.F., and Dong, X. (1994). A mutation in *Arabidopsis* that leads to constitutive expression of systemic acquired resistance. Plant Cell **6:** 1845–1857.

Boyes, D.C., Nam, J., and Dangl, J.L. (1998). The Arabidopsis thaliana RPM1 disease resistance gene product is a peripheral plasma membrane protein that is degraded coincident with the hypersensitive response. Proc. Natl. Acad. Sci. USA **95:** 15849–15854.

Burch-Smith, T.M., Schiff, M., Caplan, J.L., Tsao, J., Czymmek, K., and Dinesh-Kumar, S.P. (2007). A novel role for the TIR domain in association with pathogen-derived elicitors. PLoS Biol. **5:** e68.

Clay, N.K., Adio, A.M., Denoux, C., Jander, G., and Ausubel, F.M. (2009). Glucosinolate metabolites required for an Arabidopsis innate immune response. Science **323:** 95–101.

Collier, S.M., and Moffett, P. (2009). NB-LRRs work a "bait and switch" on pathogens. Trends Plant Sci. **14:** 521–529.

Collins, N.C., Thordal-Christensen, H., Lipka, V., Bau, S., Kombrink, E., Qiu, J.L., Huckelhoven, R., Stein, M., Freialdenhoven, A., Somerville, S.C., and Schulze-Lefert, P. (2003). SNARE-protein-mediated disease resistance at the plant cell wall. Nature **425:** 973–977.

Cooley, M.B., Pathirana, S., Wu, H.J., Kachroo, P., and Klessig, D.F. (2000). Members of the Arabidopsis *HRT*/*RPP8* family of resistance genes confer resistance to both viral and oomycete pathogens. Plant Cell **12:** 663–676.

Czechowski, T., Stitt, M., Altmann, T., Udvardi, M.K., and Scheible, W.R. (2005). Genome-wide identification and testing of superior reference genes for transcript normalization in Arabidopsis. Plant Physiol. **139:** 5–17.

Dangl, J.L., and Jones, J.D.G. (2001). Plant pathogens and integrated defence responses to infection. Nature **411:** 826–833.

Darsow, T., Rieder, S.E., and Emr, S.D. (1997). A multispecificity syntaxin homologue, Vam3p, essential for autophagic and biosynthetic protein transport to the vacuole. J. Cell Biol. **138:** 517–529.

del Pozo, O., Pedley, K.F., and Martin, G.B. (2004). MAPKKKalpha is a positive regulator of cell death associated with both plant immunity and disease. EMBO J. **23:** 3072–3082.

Deslandes, L., Olivier, J., Peeters, N., Feng, D.X., Khounlotham, M., Boucher, C., Somssich, I., Genin, S., and Marco, Y. (2003). Physical interaction between RRS1-R, a protein conferring resistance to bacterial wilt, and PopP2, a type III effector targeted to the plant nucleus. Proc. Natl. Acad. Sci. USA **100:** 8024–8029.

Dodds, P.N., Lawrence, G.J., Catanzariti, A.M., Teh, T., Wang, C.I., Ayliffe, M.A., Kobe, B., and Ellis, J.G. (2006). Direct protein interaction underlies gene-for-gene specificity and coevolution of the flax resistance genes and flax rust avirulence genes. Proc. Natl. Acad. Sci. USA **103:** 8888–8893.

Dutta, R., and Inouye, M. (2000). GHKL, an emergent ATPase/kinase superfamily. Trends Biochem. Sci. **25:** 24–28.

Field, B., Jordan, F., and Osbourn, A. (2006). First encounters–Deployment of defence-related natural products by plants. New Phytol. **172:** 193–207.

Flor, H.H. (1971). Current status of the gene-for-gene concept. Annu. Rev. Phytopathol. **9:** 275–296.

Goodin, M.M., Zaitlin, D., Naidu, R.A., and Lommel, S.A. (2008). *Nicotiana benthamiana*: Its history and future as a model for plant-pathogen interactions. Mol. Plant Microbe Interact. **21:** 1015–1026.

Grant, M., Brown, I., Adams, S., Knight, M., Ainslie, A., and Mansfield, J. (2000). The *RPM1* plant disease resistance gene facilitates a rapid and sustained increase in cytosolic calcium that is necessary for the oxidative burst and hypersensitive cell death. Plant J. **23:** 441–450.

Han, L., Dias Figueiredo, M., Berghorn, K.A., Iwata, T.N., Clark-Campbell, P.A., Welsh, I.C., Wang, W., O'Brien T.P., Lin, D.M., and Roberson, M.S. (2007). Analysis of the gene regulatory program induced by the homeobox transcription factor distal-less 3 in mouse placenta. Endocrinology **148:** 1246–1254.

Holt III, B.F., Belkhadir, Y., and Dangl, J.L. (2005). Antagonistic control of disease resistance protein stability in the plant immune system. Science **309:** 929–932.

Honda, K., Ohba, Y., Yanai, H., Negishi, H., Mizutani, T., Takaoka, A., Taya, C., and Taniguchi, T. (2005). Spatiotemporal regulation of MyD88-IRF-7 signalling for robust type-I interferon induction. Nature **434:** 1035–1040.

Hubert, D.A., He, Y., McNulty, B.C., Tornero, P., and Dangl, J.L. (2009). Specific Arabidopsis HSP90.2 alleles recapitulate RAR1 cochaperone function in plant NB-LRR disease resistance protein regulation. Proc. Natl. Acad. Sci. USA **106:** 9556–9563.

Hubert, D.A., Tornero, P., Belkhadir, Y., Krishna, P., Takahashi, A., Shirasu, K., and Dangl, J.L. (2003). Cytosolic HSP90 associates with and modulates the Arabidopsis RPM1 disease resistance protein. EMBO J. **22:** 5679–5689.

Husebye, H., Halaas, O., Stenmark, H., Tunheim, G., Sandanger, O., Bogen, B., Brech, A., Latz, E., and Espevik, T. (2006). Endocytic pathways regulate Toll-like receptor 4 signaling and link innate and adaptive immunity. EMBO J. **25:** 683–692.

Irizarry, R.A., Bolstad, B.M., Collin, F., Cope, L.M., Hobbs, B., and Speed, T.P. (2003). Summaries of Affymetrix GeneChip probe level data. Nucleic Acids Res. **31:** e15.

Jeong, R.D., Chandra-Shekara, A.C., Kachroo, A., Klessig, D.F., and Kachroo, P. (2008). HRT-mediated hypersensitive response and resistance to Turnip Crinkle Virus in Arabidopsis does not require the function of TIP, the presumed guardee protein. Mol. Plant Microbe Interact. **21:** 1316–1324.

Jia, Y., McAdams, S.A., Bryan, G.T., Hershey, H.P., and Valent, B. (2000). Direct interaction of resistance gene and avirulence gene products confers rice blast resistance. EMBO J. **19:** 4004–4014.

Kalde, M., Nuhse, T.S., Findlay, K., and Peck, S.C. (2007). The syntaxin SYP132 contributes to plant resistance against bacteria and

secretion of pathogenesis-related protein 1. Proc. Natl. Acad. Sci. USA **104:** 11850–11855.

Kang, H.G., Kuhl, J.C., Kachroo, P., and Klessig, D.F. (2008). CRT1, an Arabidopsis ATPase that interacts with diverse resistance proteins and modulates disease resistance to Turnip Crinkle Virus. Cell Host Microbe **3:** 48–57.

Kim, Y.J., Lin, N.C., and Martin, G.B. (2002). Two distinct Pseudomonas effector proteins interact with the Pto kinase and activate plant immunity. Cell **109:** 589–598.

Knight, M.R., Campbell, A.K., Smith, S.M., and Trewavas, A.J. (1991). Transgenic plant aequorin reports the effects of touch and cold-shock and elicitors on cytoplasmic calcium. Nature **352:** 524–526.

Knight, H., and Knight, M.R. (1995). Recombinant aequorin methods for intracellular calcium measurement in plants. Methods Cell Biol. **49:** 201–216.

Larsson, C., Widell, S., and Kjekkbom, P. (1987). Preparation of high-purity plasma membranes. Methods Enzymol. **148:** 558–568.

Lecourieux, D., Mazars, C., Pauly, N., Ranjeva, R., and Pugin, A. (2002). Analysis and effects of cytosolic free calcium increases in response to elicitors in *Nicotiana plumbaginifolia* cells. Plant Cell **14:** 2627–2641.

Leipe, D.D., Koonin, E.V., and Aravind, L. (2004). STAND, a class of P-loop NTPases including animal and plant regulators of programmed cell death: Multiple, complex domain architectures, unusual phyletic patterns, and evolution by horizontal gene transfer. J. Mol. Biol. **343:** 1–28.

Leister, R.T., Dahlbeck, D., Day, B., Li, Y., Chesnokova, O., and Staskawicz, B.J. (2005). Molecular genetic evidence for the role of SGT1 in the intramolecular complementation of Bs2 protein activity in *Nicotiana benthamiana.* Plant Cell **17:** 1268–1278.

Li, L., He, Z., Pandey, G.K., Tsuchiya, T., and Luan, S. (2002). Functional cloning and characterization of a plant efflux carrier for multidrug and heavy metal detoxification. J. Biol. Chem. **277:** 5360–5368.

Liu, Y., Schiff, M., and Dinesh-Kumar, S.P. (2002a). Virus-induced gene silencing in tomato. Plant J. **31:** 777–786.

Liu, Y., Schiff, M., Marathe, R., and Dinesh-Kumar, S.P. (2002b). Tobacco Rar1, EDS1 and NPR1/NIM1 like genes are required for N-mediated resistance to tobacco mosaic virus. Plant J. **30:** 415–429.

Lu, R., Malcuit, I., Moffett, P., Ruiz, M.T., Peart, J., Wu, A.J., Rathjen, J.P., Bendahmane, A., Day, L., and Baulcombe, D.C. (2003). High throughput virus-induced gene silencing implicates heat shock protein 90 in plant disease resistance. EMBO J. **22:** 5690–5699.

Mackey, D., Belkhadir, Y., Alonso, J.M., Ecker, J.R., and Dangl, J.L. (2003). Arabidopsis RIN4 is a target of the type III virulence effector AvrRpt2 and modulates RPS2-mediated resistance. Cell **112:** 379–389.

Mackey, D., Holt III, B.F., Wiig, A., and Dangl, J.L. (2002). RIN4 interacts with *Pseudomonas syringae* type III effector molecules and is required for RPM1-mediated resistance in Arabidopsis. Cell **108:** 743–754.

Martin, G.B., Bogdanove, A.J., and Sessa, G. (2003). Understanding the functions of plant disease resistance proteins. Annu. Rev. Plant Biol. **54:** 23–61.

Martin, G.B., Brommonschenkel, S.H., Chunwongse, J., Frary, A., Ganal, M.W., Spivey, R., Wu, T., Earle, E.D., and Tanksley, S.D. (1993). Map-based cloning of a protein kinase gene conferring disease resistance in tomato. Science **262:** 1432–1436.

Martinon, F., Mayor, A., and Tschopp, J. (2009). The inflammasomes: Guardians of the body. Annu. Rev. Immunol. **27:** 229–265.

McDowell, J.M., Dhandaydham, M., Long, T.A., Aarts, M.G., Goff, S., Holub, E.B., and Dangl, J.L. (1998). Intragenic recombination and diversifying selection contribute to the evolution of downy mildew resistance at the *RPP8* locus of Arabidopsis. Plant Cell **10:** 1861–1874.

McDowell, J.M., Williams, S.G., Funderburg, N.T., Eulgem, T., and Dangl, J.L. (2005). Genetic analysis of developmentally regulated resistance to downy mildew (*Hyaloperonospora parasitica*) in *Arabidopsis thaliana*. Mol. Plant Microbe Interact. **18:** 1226–1234.

Menke, F.L., van Pelt, J.A., Pieterse, C.M., and Klessig, D.F. (2004). Silencing of the mitogen-activated protein kinase MPK6 compromises disease resistance in *Arabidopsis*. Plant Cell **16:** 897–907.

Mindrinos, M., Katagiri, F., Yu, G.L., and Ausubel, F.M. (1994). The *A. thaliana* disease resistance gene RPS2 encodes a protein containing a nucleotide-binding site and leucine-rich repeats. Cell **78:** 1089–1099.

Mucyn, T.S., Clemente, A., Andriotis, V.M., Balmuth, A.L., Oldroyd, G.E., Staskawicz, B.J., and Rathjen, J.P. (2006). The tomato NBARC-LRR Protein Prf interacts with Pto kinase in vivo to regulate specific plant immunity. Plant Cell **18:** 2792–2806.

Nagahashi, J., and Hiraike, K. (1982). Effects of centrifugal force and centrifugation time on the sedimentation of plant organelles. Plant Physiol. **69:** 546–548.

Nawrath, C., Heck, S., Parinthawong, N., and Metraux, J.P. (2002). EDS5, an essential component of salicylic acid-dependent signaling for disease resistance in *Arabidopsis*, is a member of the MATE transporter family. Plant Cell **14:** 275–286.

Nelson, B.K., Cai, X., and Nebenfuhr, A. (2007). A multicolored set of in vivo organelle markers for co-localization studies in Arabidopsis and other plants. Plant J. **51:** 1126–1136.

Ong, L.E., and Innes, R.W. (2006). AvrB mutants lose both virulence and avirulence activities on soybean and Arabidopsis. Mol. Microbiol. **60:** 951–962.

Page, M.D., Kropat, J., Hamel, P.P., and Merchant, S.S. (2009). Two *Chlamydomonas* CTR copper transporters with a novel Cys-Met motif are localized to the plasma membrane and function in copper assimilation. Plant Cell **21:** 928–943.

Pratt, W.B., and Toft, D.O. (2003). Regulation of signaling protein function and trafficking by the hsp90/hsp70-based chaperone machinery. Exp. Biol. Med. **228:** 111–133.

Rairdan, G., and Moffett, P. (2007). Brothers in arms? Common and contrasting themes in pathogen perception by plant NB-LRR and animal NACHT-LRR proteins. Microbes Infect. **9:** 677–686.

Rairdan, G.J., Collier, S.M., Sacco, M.A., Baldwin, T.T., Boettrich, T., and Moffett, P. (2008). The coiled-coil and nucleotide binding domains of the Potato Rx disease resistance protein function in pathogen recognition and signaling. Plant Cell **20:** 739–751.

Redman, J.C., Haas, B.J., Tanimoto, G., and Town, C.D. (2004). Development and evaluation of an Arabidopsis whole genome Affymetrix probe array. Plant J. **38:** 545–561.

Ren, T., Qu, F., and Morris, T.J. (2000). *HRT* gene function requires interaction between a NAC protein and viral capsid protein to confer resistance to Turnip Crinkle Virus. Plant Cell **12:** 1917–1926.

Ren, T., Qu, F., and Morris, T.J. (2005). The nuclear localization of the Arabidopsis transcription factor TIP is blocked by its interaction with the coat protein of *Turnip crinkle virus.* Virology **331:** 316–324.

Reuveni, M., Evenor, D., Artzi, B., Perl, A., and Erner, Y. (2001). Decrease in vacuolar pH during petunia flower opening is reflected in the activity of tonoplast H+-ATPase. J. Plant Physiol. **158:** 991–998.

Sacco, M.A., Mansoor, S., and Moffett, P. (2007). A RanGAP protein physically interacts with the NB-LRR protein Rx, and is required for Rx-mediated viral resistance. Plant J. **52:** 82–93.

Salmeron, J.M., Oldroyd, G.E., Rommens, C.M., Scofield, S.R., Kim, H.S., Lavelle, D.T., Dahlbeck, D., and Staskawicz, B.J. (1996). Tomato *Prf* is a member of the leucine-rich repeat class of plant disease resistance genes and lies embedded within the *Pto* kinase gene cluster. Cell **86:** 123–133.

Sato, M., Mitra, R.M., Coller, J., Wang, D., Spivey, N.W., Dewdney, J., Denoux, C., Glazebrook, J., and Katagiri, F. (2006). A high-performance, small-scale microarray for expression profiling of many samples in Arabidopsis-pathogen studies. Plant J. **49:** 565–577.

Schechter, L.M., Roberts, K.A., Jamir, Y., Alfano, J.R., and Collmer, A. (2004). *Pseudomonas syringae* type III secretion system targeting signals and novel effectors studied with a Cya translocation reporter. J. Bacteriol. **186:** 543–555.

Schmittgen, T.D., and Livak, K.J. (2008). Analyzing real-time PCR data by the comparative C(T) method. Nat. Protoc. **3:** 1101–1108.

Schwessinger, B., and Zipfel, C. (2008). News from the frontline: recent insights into PAMP-triggered immunity in plants. Curr. Opin. Plant Biol. **11:** 389–395.

Scofield, S.R., Tobias, C.M., Rathjen, J.P., Chang, J.H., Lavelle, D.T., Michelmore, R.W., and Staskawicz, B.J. (1996). Molecular basis of gene-for-gene specificity in bacterial speck disease of tomato. Science **274:** 2063–2065.

Sekine, K.T., Ishihara, T., Hase, S., Kusano, T., Shah, J., and Takahashi, H. (2006). Single amino acid alterations in *Arabidopsis thaliana* RCY1 compromise resistance to Cucumber mosaic virus, but differentially suppress hypersensitive response-like cell death. Plant Mol. Biol. **62:** 669–682.

Shaner, N.C., Campbell, R.E., Steinbach, P.A., Giepmans, B.N., Palmer, A.E., and Tsien, R.Y. (2004). Improved monomeric red, orange and yellow fluorescent proteins derived from Discosoma sp. red fluorescent protein. Nat. Biotechnol. **22:** 1567–1572.

Shao, F., Golstein, C., Ade, J., Stoutemyer, M., Dixon, J.E., and Innes, R.W. (2003). Cleavage of Arabidopsis PBS1 by a bacterial type III effector. Science **301:** 1230–1233.

Shaw, A.S., and Filbert, E.L. (2009). Scaffold proteins and immune-cell signalling. Nat. Rev. Immunol. **9:** 47–56.

Shen, Q.H., Saijo, Y., Mauch, S., Biskup, C., Bieri, S., Keller, B., Seki, H., Ulker, B., Somssich, I.E., and Schulze-Lefert, P. (2007). Nuclear activity of MLA immune receptors links isolate-specific and basal disease-resistance responses. Science **315:** 1098–1103.

Shirano, Y., Kachroo, P., Shah, J., and Klessig, D.F. (2002). A gain-of-function mutation in an *Arabidopsis* Toll interleukin1 receptor-nucleotide binding site-leucine-rich repeat type *R* gene triggers defense responses and results in enhanced disease resistance. Plant Cell **14:** 3149–3162.

Shirasu, K., and Schulze-Lefert, P. (2003). Complex formation, promiscuity and multi-functionality: Protein interactions in disease-resistance pathways. Trends Plant Sci. **8:** 252–258.

Surpin, M., and Raikhel, N. (2004). Traffic jams affect plant development and signal transduction. Nat. Rev. Mol. Cell Biol. **5:** 100–109.

Tameling, W.I., Elzinga, S.D., Darmin, P.S., Vossen, J.H., Takken, F.L., Haring, M.A., and Cornelissen, B.J. (2002). The tomato *R* gene products I-2 and MI-1 are functional ATP binding proteins with ATPase activity. Plant Cell **14:** 2929–2939.

Tameling, W.I., Vossen, J.H., Albrecht, M., Lengauer, T., Berden, J.A., Haring, M.A., Cornelissen, B.J., and Takken, F.L. (2006). Mutations in the NB-ARC domain of I-2 that impair ATP hydrolysis cause autoactivation. Plant Physiol. **140:** 1233–1245.

Tamura, K., Dudley, J., Nei, M., and Kumar, S. (2007). MEGA4: Molecular Evolutionary Genetics Analysis (MEGA) software version 4.0. Mol. Biol. Evol. **24:** 1596–1599.

Tang, X., Frederick, R.D., Zhou, J., Halterman, D.A., Jia, Y., and Martin, G.B. (1996). Initiation of plant disease resistance by physical interaction of AvrPto and Pto kinase. Science **274:** 2060–2063.

Tao, Y., Xie, Z., Chen, W., Glazebrook, J., Chang, H.S., Han, B., Zhu, T., Zou, G., and Katagiri, F. (2003). Quantitative nature of *Arabidopsis* responses during compatible and incompatible interactions with the bacterial pathogen *Pseudomonas syringae.* Plant Cell **15:** 317–330.

Tao, Y., Yuan, F., Leister, R.T., Ausubel, F.M., and Katagiri, F. (2000). Mutational analysis of the *Arabidopsis* nucleotide binding site-leucine-rich repeat resistance gene *RPS2.* Plant Cell **12:** 2541–2554.

van der Hoorn, R.A., and Kamoun, S. (2008). From guard to decoy: A new model for perception of plant pathogen effectors. Plant Cell **20:** 2009–2017.

Wang, D., Weaver, N.D., Kesarwani, M., and Dong, X. (2005). Induction of protein secretory pathway is required for systemic acquired resistance. Science **308:** 1036–1040.

Wang, Y., Gao, M., Li, Q., Wang, L., Wang, J., Jeon, J.S., Qu, N., Zhang, Y., and He, Z. (2008). OsRAR1 and OsSGT1 physically interact and function in rice basal disease resistance. Mol. Plant Microbe Interact. **21:** 294–303.

Weaver, L.M., Swiderski, M.R., Li, Y., and Jones, J.D. (2006). The *Arabidopsis thaliana* TIR-NB-LRR R-protein, RPP1A; Protein localization and constitutive activation of defence by truncated alleles in tobacco and Arabidopsis. Plant J. **47:** 829–840.

Wirthmueller, L., Zhang, Y., Jones, J.D., and Parker, J.E. (2007). Nuclear accumulation of the Arabidopsis immune receptor RPS4 is necessary for triggering EDS1-dependent defense. Curr. Biol. **17:** 2023–2029.

Wu, Z., Irizarry, R.A., Gentleman, R., Murillo, F.M., and Spencer, F. (2004). A model based background adjustment for oligonucleotide expression arrays. J. Am. Stat. Assoc. **99:** 909–917.

Xiao, F., He, P., Abramovitch, R.B., Dawson, J.E., Nicholson, L.K., Sheen, J., and Martin, G.B. (2007). The N-terminal region of Pseudomonas type III effector AvrPtoB elicits Pto-dependent immunity and has two distinct virulence determinants. Plant J. **52:** 595–614.

Yang, K.Y., Liu, Y., and Zhang, S. (2001). Activation of a mitogen-activated protein kinase pathway is involved in disease resistance in tobacco. Proc. Natl. Acad. Sci. USA **98:** 741–746.

Zhao, Y., DelGrosso, L., Yigit, E., Dempsey, D.A., Klessig, D.F., and Wobbe, K.K. (2000). The amino terminus of the coat protein of Turnip Crinkle Virus is the Avr factor recognized by resistant Arabidopsis. Mol. Plant Microbe Interact. **13:** 1015–1018.

Zuo, J., Niu, Q.W., and Chua, N.H. (2000). An estrogen receptor-based transactivator XVE mediates highly inducible gene expression in transgenic plants. Plant J. **24:** 265–273.